JPRS-UMS-92-017
10 December 1992

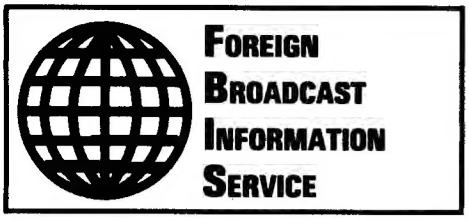

JPRS Report

Science & Technology

Central Eurasia: Materials Science

Science & Technology
Central Eurasia: Materials Science

JPRS-UMS-92-017 CONTENTS 10 December 1992

Analysis, Testing

Coatings

Corrosion

Ferrous Metals

Nonferrous Metals, Alloys, Brazes, Solders

Nonmetallic Materials

Preparations

Treatments

Welding, Brazing, Soldering

Extractive Metallurgy, Mining

Cracking Resistance of Chromium-Nickel Steels During Impact Loading at Cryogenic Temperatures

937D0004A Kiev PROBLEMY PROCHNOSTI in Russian No 7, Jul 1992 pp 26-28

[Article by O. Ya. Znachkovskiy, M. A. Izarov, and Yu. A. Kolomnets, Institute of Strength Problems of the Ukrainian Academy of Sciences, Kiev; UDC 620.178.7]

[Abstract] The resistance of 12Kh18N10T and 03Kh20N16AG6 chromium-nickel steels to cracking during impact loading at cryogenic temperatures was investigated. Standard three-point bending tests were performed on a pendulum-type impact tester equipped with an electronic device utilized to record the deformation curves generated during testing. The device was designed by the Institute of Strength Problems. The loading rate was about 1.5 m/s. To measure the load, strain sensors were glued to the end of the impacter, the motion of which was recorded by a photosensor. Test specimens 12 x 24 x 120 mm in size were made from 03Kh20N16AG6 sheet steel 16 mm thick, and specimens 10 x 24 x 120 mm in size were made from 12Kh18N10T sheet steel 11 mm thick. These specimens were made with an initial fatigue crack. Tests were also performed on notched specimens 10 x 10 x 55 mm in size with notch apex radii of 1 and 0.25 mm (types I and II per GOST 9454—78). The notches were made so that the cracks would run across the direction in which the steel was rolled. Testing was done at temperatures ranging from 293 to 77 K by first immersing the specimens in ethyl alcohol cooled with liquid nitrogen for at least five minutes, then immersing them directly in liquid nitrogen. The results, which were analyzed using non-linear failure mechanics methods, showed that the cracking resistance of the 03Kh20N16AG6 steel begins to deteriorate at temperatures below 178 K, and its impact toughness gradually deteriorates throughout the entire range of temperatures tested. The cracking resistance of the 12Kh18N10T steel begins to deteriorate at temperatures above 178 K. However, the 12Kh18N10T steel still has greater cracking resistance during impact loading than the 03Kh20N16AG6 steel throughout the entire range of temperatures tested. Figures 3; references 3: Russian.

Effect of Loading Rate and Temperature on the Cracking Resistance of Structural Steels

937D0004B Kiev PROBLEMY PROCHNOSTI in Russian No 7, Jul 1992 pp 30-33

[Article by A. V. Viklin, Yu. P. Solnstev, and V. V. Skobkin, Institute of Refrigeration Technology, St. Petersburg; UDC 539.4]

[Abstract] Standard procedures were used to test a number of different structural steels for static and dynamic cracking resistance, and the resulting data were utilized to develop a quantitative method for estimating what the cracking resistance and load-bearing capacity of these steels would be under service conditions. The steels tested were 30KhMA, 35KhMFA, 38KhMA, 38Kh2N2MA, 35L, and 40L. The steels underwent different heat-treating processes, and as a result had widely differing grain sizes, grain structures, and mechanical properties. The static cracking resistance was tested on an Instron-1255 using compact specimens 25 and 50 mm thick. These data were used to calculate the critical coefficients for stress intensity and for stress intensity at maximum load. Dynamic cracking resistance during bending at a rate of about 6 m/s was tested using specimens 10 mm thick on an RD 50-344-82 in conjunction with an oscillograph. The experimental data were used to generate curves showing cracking resistance as a function of temperature during static and dynamic loading. The curves were generalized by using a normalized temperature that reflected the critical temperature corresponding to a 50 percent viscous component in the type of fracture induced in a standard deeply notched Charpy impact test specimen. The study showed that these types of curves, when used in conjunction with inequalities characterizing a material's inherent and structural cracking resistance, can be successfully used to estimate the cracking resistance and load-carrying capacity of structural steels under service conditions. Figures 2, tables 1; references 6: Russian.

Tool Material Strength During Single Impact Loading

937D0004C Kiev PROBLEMY PROCHNOSTI in Russian No 7, Jul 1992 pp 33-40

[Article by L. N. Devin and M. D. Vaysband, Institute of Superhard Materials of the Ukrainian Academy of Sciences, Kiev; UDC 539.4]

[Abstract] New testing equipment and procedures were developed to test the strength and cracking resistance of brittle tool materials during single impact loading. The new testing apparatus features an improved preamplifier with a low level of free noise, a wide frequency range, a stabilized power supply for the strain sensors, a wide dynamic range, and an amplification factor of 400-500. As the dynamic component of measurement error for this equipment is rather large, test procedures and results were adjusted accordingly, with the aid of a special auxiliary computing device. When the new equipment was used to test six tungsten-cobalt hard alloys, the results showed that bending strength and cracking resistance increased when loading was changed from static to dynamic and that cracking resistance increased substantially when the loading rate was increased from 50 to 1000- 10,000 mm/min. During static loading, the cracking resistance of hard alloys with high-temperature tungsten carbide increased as the cobalt phase percentage and grain size increased, but hardness decreased. However, this should not affect the wear resistance of these alloys, as the decrease in hardness would be offset by the higher cracking resistance, provided there is an optimum trade-off between the two properties. The cracking resistance of these materials was also higher

during dynamic than during static loading. The strength of a number of polycrystals of superhard materials and ceramics during dynamic loading was also tested, and the results used to sort the materials into three types: those which increased in strength during dynamic loading, one which decreased in strength under dynamic loading, and those which were largely unaffected. Kiborite had the greatest strength of all the materials tested under dynamic loads. During static loading, amborite was the strongest of the superhard materials, and cortinite was the strongest of the ceramics. Figures 6, tables 2; references 9: Russian.

Structure and Mechanical Properties of Cu-Al Alloys Subjected to Impact Compression

937D0004D Kiev PROBLEMY PROCHNOSTI in Russian No 7, Jul 1992 pp 44-48

[Article by G. I. Shakhalova and A. I. Yevplov, Pedagogical Institute, Nizhniy Novgorod; UDC 539.4]

[Abstract] Two Cu-Al alloys with different stacking fault energies were studied to determine the relationship between this energy, transverse sliding, and twinning during plastic deformation. Alloy I (Cu + 1.64 wt. percent Al) had a stacking fault energy of 20 mJ/sq m. For Alloy II (Cu + 6.07 wt. percent Al), this quantity was 2 mJ/sq m. Both alloys were single-phase with a face-centered cubic lattice. Heat treating was employed to achieve a uniform grain size of 0.1 mm in both alloys. The alloys were subjected to 40 and 60 microseconds of impact compressive loading, which was effected by the Kolskiy method, using a Hopkinson rod. Maximum effective stress fell between 600 and 650 MPa. Statistical analysis of the test data, which was quite scattered, showed that when the concentration of Al in the alloy was increased, stacking fault energy decreased. The decrease in stacking fault energy impeded the twinning process during impact compressive loading. Consequently, twinning played a much smaller role than the sliding mechanism in the plastic deformation of Alloy II than in Alloy I, in which the two mechanisms are known to compete. The test data were borne out by metallographic and radiographic analyses. Figures 2, tables 3; references 2: Russian.

Effect of Pulse Loading on Creep in Damaged Steam Pipe

937D0004E Kiev PROBLEMY PROCHNOSTI in Russian No 7, Jul 1992 pp 56-59

[Article by A. N. Olnsov and A. V. Maslakov, Institute of Strength Problems of the Ukrainian Academy of Sciences, Kiev; UDC 539.4:620.17]

[Abstract] Specimens of damaged 12Kh1MF steel were subjected to pulse loading in order to determine its effect on hardness, long-term strength, and creep. The 14 x 14 x 130 mm specimens were fashioned from sections of steam pipe showing signs of wear and tear after 130,000 hours of service during which the pipe was exposed to a temperature of 540° C and an internal pressure of 10 MPa. The specimens were made so that their long sides corresponded to the longitudinal axis of the pipe. Pulse loading was effected transversely by striking the specimen with a vertical pneumatic vacuum impacter made of St. 3 steel weighing 1 kg and moving at 94 m/s, with the specimen placed on a flexible semi-infinite base of St. 3 steel. The specimens were tested for hardness (Vickers hardness on a TP-7r-1 tester), strength, and creep using standard methods and equipment before and after loading. It was shown that all three properties increased substantially after pulse loading. Hardness increased by an average of 22 percent, from 1.39 GPa before loading to 1.70 GPa after loading. Long-term strength at 156 MPa at 540° C increased from 146 hours to rupture before loading to 276 hours to rupture after loading, and the creep rate fell from 13.2×10^{-2} percent per hour to 3.6×10^{-2} percent per hour. The effect was even more dramatic under a 130-MPa test load: Strength increased 2.2-fold, and creep resistance 4.4-fold. Similar tests performed on damaged specimens of Al + 6 percent Mg yielded similarly positive results. Figures 2, tables 1, references 8: Russian.

Ultimate State of Thin-Walled Tube Deformed by Longitudinal Force, Torque, and Internal Pressure

937D0004F Kiev PROBLEMY PROCHNOSTI in Russian No 7, Jul 1992 pp 59-63

[Article by S. A. Yelsufyev, Odessa, Civil Engineering Institute; UDC 539.376]

[Abstract] A criterion of infinite elongation rate at the moment of elongation localization was used in conjunction with rheological equations that account for large creep deformations, the type of stressed state, and damage susceptibility to develop deformation equations that can be used to predict the ultimate state of thin-walled tube exposed to longitudinal force, torque, and internal pressure. The adduced correlations generalize known criteria for plastic stability when affected by the type of stressed state and by the exponent of the law of strengthening and damage susceptibility. The results generated by the equations comported with the validating experimental data. Figures 1, references 8: 6 Russian, 2 Western.

Using Ion Implantation To Modify the Microstructure and Mechanical Properties of Metals and Alloys

937D0005A Moscow POVERHKNOST: FIZIKA, KHIMIYA, MEKHANIKA in Russian No 7, Aug 1992 pp 5-20

[Article by Z. A. Iskanderova, T. D. Radzhabov, and G. R. Rakhimova, Institute of Electronics of the Uzbek Academy of Sciences, Tashkent; UDC 620.197]

[Abstract] Studies on the use of ion implantation to modify the microstructure and mechanical properties of

metals and their alloys were surveyed. The survey was comprehensive and covered research that has been carried out over the past five to 10 years by both Soviet and non-Soviet scientists and that has been published and/or presented at conferences. The findings of these studies, which were systematically analyzed and presented in the survey, showed that ion bombardment with chemically active gas ions, particularly those of nitrogen, is the most effective way to increase microhardness, wear-resistance, and endurance (as measured by fatigue testing), and to reduce the coefficient of friction. Ion implantation conditions and practices and subsequent heat treatment substantially affect the distribution, total concentration, and phase composition of alloying elements and, consequently, the modification of the microstructure and tribological properties of materials surfaces as a result of the introduction of chemically active impurities. It is thought that the most probable causes of this process are the solid dispersed precipitations of the new phase, the formation of a multi-phase zone, and the migration of the implanted ions deep into the matrix during friction due to the thermomechanical effect, as well as by the presence of a developed dislocation structure induced by the radiation and by the formation of "contaminated" subsurface layers (oxide, carbon, etc.) due to the vacuum conditions that prevail during high-flux ion implantation. Figures 10, tables 5; references 46: 15 Russian, 31 Western.

Electron Density of States in Small Metal Particles and Thin Films With Surface Defects

937D0005B Moscow POVERHKNOST: FIZIKA, KHIMIYA, MEKHANIKA in Russian No 7, Aug 1992 pp 30-36

[Article by E. P. Nagayev; UDC 539.21]

[Abstract] The effect of surface defects, primarily in the form of vacancies and adsorbed atoms, on electron density of states, Fermi energy, and electron surface energy was studied in small metal particles and thin films of regular shape. The Green function and the Euler-MacLoren equation were used together to calculate coarse-grained electron state densities. The spatial quantization in coarse-grained densities is "remembered" by adding a term proportional to the surface area to the usual bulk density of states. The calculations showed that the contribution of the defects to the surface density of states increases as energy is decreased, while at the same time, its ideal portion does not depend on energy. Thus, for low Fermi energy values, the contribution of defects to the surface density of states can greatly exceed their relative concentration. At low electron densities, this contribution can exceed the relative concentration of vacancies and adatoms by at least one order of magnitude. A qualitatively new finding of this study is that, because the number of adatoms is a function of temperature, coarse-grained density is also a function of temperature. This relationship leads, for example, to a relationship between temperature and the magnetic susceptibility of the conductivity electrons. If the natural spin of the adatoms is equal to zero, than the susceptibility of a paramagnetic metal can be the only cause of this relationship. References 9: 7 Russian, 2 Western.

Using Pulsed Laser Radiation of Nanosecond Duration To Modify the Structure of Porous Silicon Layers

937D0005C Moscow POVERHKNOST: FIZIKA, KHIMIYA, MEKHANIKA in Russian No 7, Aug 1992 pp 44-49

[Article by S. A. Batishche, V. I. Bondarenko, A. V. Demchuk, A. A. Kuzmuk, V. A. Labunov, G. V. Litvinovich, V. A. Mostovnikov, and G. A. Tatur, Institute of Physics of the Belorusian Academy of Sciences, Minsk, and the Minsk Radio Engineering Institute; UDC 621.315.592]

[Abstract] The use of pulsed laser radiation to recrystallize layers of porous silicon into single-crystal layers was studied. Silicon wafers underwent galvanostatic anodizing in a 12 percent aqueous HF solution at room temperature to produce specimens that were 3 μm thick and that had porosities of 10, 30, and 50 percent. The specimen surfaces were exposed to 50-ns pulsed radiation with a wave length of 0.53 μm and a power density of 0.1-2 j/sq cm produced by an Nd-glass Q-switched laser operating at room temperature in atmospheric air. The angle of radiation incidence to the specimen surfaces was normal. The results of time-resolved optical probing and of optical, scanning electron, and transmission electron microscopy showed that, due to the inverse relationship between porosity and thermal conductivity, an increase in radiation power density leads to an increase in the lifespan of the liquid phase and, consequently, to a lower thermal gradient and the overcooling of the entire melted layer. Under these conditions, nucleation begins to occur at the interphase boundary, on the surface of the layer, and in the layer itself, and surface tension leads to the creation of drop-shaped regions at the solid-liquid interface. The crystallization of these regions leads to the formation of individual grains that are not part of the underlying structure. Thus, within a power density range of 0.46 to 0.9 J/sq cm, where this mechanism is absent, the epitaxial crystallization of the melt layer takes place, resulting in the formation of a recrystallized silicon layer that is about 0.5 μm thick when the power density is 0.9 J/sq cm. Figures 4; references 6: 2 Russian, 4 Western.

Relationship Between the Structure and Optical Properties of Polypropylene Modified by Fluorine Ion Implantation

937D0005D Moscow POVERHKNOST: FIZIKA, KHIMIYA, MEKHANIKA in Russian No 7, Aug 1992 pp 113-117

[Article by O. Yu. Posudiyevskiy, I. G. Myasnikova, and A. A. Chuyko, Institute of Surface Chemistry of the Ukrainian Academy of Sciences, Kiev; UDC 678.7:621.315.5]

[Abstract] Polypropylene modified by the implantation of 50 keV fluorine ions was studied to determine the relationship between the modified structure and the optical properties of the material. The formation of the modified structure took place in three successive stages. The first stage, which occurred until the implantation dose reached approximately 5 x 10^{14}F+/sq cm, was marked by the intensive formation of a solid chain structure of material characterized by the formation of aromatic structures. The next stage consisted of the condensation of the benzene rings into clusters of varying shape, the size of which increased in proportion to the implantation dose. During the third stage, when the implantation dose reached at least 10^{17}F+/sq cm, the condensation process continued to take place and was accompanied by the destruction of some of the π-clusters. The optical properties of the modified polymer were measured with an M-40 spectrophotometer. The absorption coefficient α as a function of photon energy was shown to conform to Tauc's law and to be determined by the electron transitions between the allowed zones of the condensed benzene ring clusters formed as a result of implantation. The presence of an optical gap signified that the aromatic nature of the electron states does not percolate throughout the entire specimen, thus indicating the presence of π-cluster islets within the compact clusters of condensed benzene rings constituting the principal structural elements of the modified polymer. As polypropylene macromolecules have a relatively simple composition and structure, this process is probably universal for all polymers modified by fluorine ion implantation. Figures 2, tables 1; references 10: 3 Russian, 7 Western.

Photoinjection Processes in the Structure of the Si- $Ba_{0.9}Sr_{0.1}TiO_3$ System

937D0005E Moscow POVERHKNOST: FIZIKA, KHIMIYA, MEKHANIKA in Russian No 7, Aug 1992 pp 124-127

[Article by A. G. Petrukhin and A. V. Petrov, Department of Physics, Moscow State University imeni M. V. Lomonosov; UDC 621.315.592]

[Abstract] Photoinjection processes were studied in a Si-ferroelectric system made by the reactive high-frequency sputtering of a $Ba_{0.9}Sr_{0.1}TiO_3$ film 0.8 μm thick onto the surface of an actual n-type silicon single crystal in an oxygen environment. Control specimens were made by applying the ferroelectric film to Si crystals that had a SiO_2 layer 1.5 μm thick. The FE films had a fine- grained polycrystalline structure and a Curie temperature of 355 K. The photoinjection processes were studied by optically charging the dielectric film. The corresponding optical charge spectra were taken as the quantum energy was gradually increased from 1.2 to 5.8 eV in 0.2-eV intervals. Exposure time for each measurement was 10^{18} quanta/sq cm. The FE film charge during exposure was measured in a 10^{-4}-Pa vacuum at 290° K by registering the change in the contact potential difference between the specimen and a gold variable electrode, using calibrated measurements to adjust for the field effect. Before each measurement, the accumulated charge was removed by either heating the specimen or keeping it at room temperature for some time. The data obtained were used to construct an energy diagram of the Si-FE structure. An energy barrier value of 1.6 eV corresponded to the bottom of the Si conductivity zone and the ceiling of the FE valency zone. The distance between this zone and the bottom of the FE conductivity zone was equal to a barrier value of 3.1 eV (the electron photoinjection threshold). The barrier value for zone-zonal generation in the FE is 3.6 eV, which provides information about the width of the FE forbidden zone. The Si-FE system was then coated with rhodamine B, which did not create additional centers for capturing photoinjected charge carriers. Figures 2; references 12: 8 Russian, 4 Western.

Dislocation Structure Evolution in High Nitrogen Austenitic Steels

937D0029B Moscow IZVESTIYA VYSSHIKH UCHEBNYKH ZAVEDENIY: CHERNAYA METALLURGIYA in Russian No 4, Apr 92 pp 34-37

[Article by N.A. Dubovik, L.B. Zuyev, Strength Physics and Materials Science Institute at the Siberian Department of the USSR Academy of Sciences, Tomsk; UDC 669.15'786-194.3:548.4]

[Abstract] The lack of data on the dislocation structure characteristics which affect the behavior of the Cr_2N precipitation during the annealing of strained nitrogen steels prompted a study of two experimental steels. To this end, ingots are annealed in the air and forged, and the samples cut from the ingots are water quenched at 1,200° C, then deformed by rolling at 20° C with a reduction degree of 20-95 percent. The metal structure is examined under Neophot-21 metallographic and EVM-100B electron microscopes after etching the sections with a mixture of acids. The structure of steels Kh17AG18 and Kh17AG18F deformed by rolling at various temperatures with various reduction degrees is cited, and the dependence of the dislocation cell size and disorientation angle on the degree of cold deformation of these two steels is plotted. The dependence of the steel substructure on the percentage reduction during cold rolling is investigated. An analysis demonstrates that the dislocation structure evolution proceeds by the following mechanism: from translational slip-twinning to formation of nondisordered cell to cell disordering to fragmentation; rotational deformation modes become involved in the stress relaxation process at a certain stage. In the absence of stress concentrators in steel Kh17AG18, transverse slip is possible at higher degrees of deformation than in steel Kh17AG18F. A change in the chromium carbide precipitation mechanism during the annealing of strained high nitrogen steel is due to the development of a cellular and cellular-fragmented dislocation structure with a $>1°$ cell and fragment disorientation. Figures 2; tables 1; references 9.

Magnetic Behavior Characteristics of Fe-Cr-Co System Alloys

937D0030F Moscow IZVESTIYA VYSSHIKH UCHEBNYKH ZAVEDENIY: CHERNAYA METALLURGIYA in Russian No 3, Mar 92 pp 46-47

[Article by V.M. Belova, B.A. Samarin, V.G. Tokarev, Moscow Steel and Alloy Institute; UDC 538.2:621.3.013]

[Abstract] The processes accompanying the formation of a highly coercive state in Fe-Cr-Co alloys, e.g., an α-solid solution stratification into high magnetic Fe-rich and low magnetic Cr-rich phases, and the presence of ferro-and antiferromagnetic phases and an abnormal behavior of the temperature drop within a 686-765K range are discussed, and an attempt is made to ascertain the nature of this anomaly. To this end, the field and temperature dependence of specific magnetization is measured in an alloy with 27 percent Cr and 12 percent Co. The specific magnetization curve of the alloy in the highly coercive state at various temperatures; the superparamagnetic contribution to the specific magnetization of the alloy as a function of the true field ratio in the sample to the absolute temperature; and the dependence of the superparamagnetic contribution on this ratio are plotted. It is speculated that the criterion of superparamagnetism is satisfied, i.e., the temperature and field dependence of the additional magnetic moment are described by Langevin's function. An analysis reveals that Langevin's model adequately describes the experimental dependence of the magnetic moment in strong fields, making it possible to attribute the abnormal temperature drop behavior to a magnetic phase transition in superparamagnetic alloy particles. Figures 2; references 2: 1 Russian, 1 Western.

Effect of Straining and Annealing on Stressed State of Ni-Based Complex Doped Superalloy

937D0030G Moscow IZVESTIYA VYSSHIKH UCHEBNYKH ZAVEDENIY: CHERNAYA METALLURGIYA in Russian No 3, Mar 92 pp 50-52

[Article by A.V. Bilchenko, V.I. Latysheva, V.A. Rafalovskiy, Kiev Polytechnic Institute and Physics of Metals Institute at the Ukrainian Academy of Sciences; UDC 669.245.018.44:621.426]

[Abstract] The poor ductility and cracking tendency of strong Ni-based superalloys is noted, and the reasons for the crack formations are discussed. The effect of the straining degree, annealing temperature, and heating rate on the properties of wire from the EI828-VD complex-doped superalloy containing 4-4.5 percent Al and 14 percent (Mo + W) is examined. The study is carried out using wire samples with a 3 mm diameter deformed with a total reduction of 10-75 percent; the samples are heated at a 1-10K/s rate in an air furnace with a three minute exposure and at a 50-160K/s rate by passing current through the wires in a commercial electric contact heating unit. The stressed state is analyzed by examining the effect of the annealing temperature and deformation degree on the alloy microhardness; second-kind microdistortions are determined at the same time by a DRON-2 diffractometer in Fe-radiation. The microhardness behavior of strained samples during heating at 1-10K/s rates, second-kind microdistortion and microhardness behavior as a function of the deformation degree, and the microhardness behavior of deformed samples under electric contact heating at a 160 K/s rate are plotted. The findings indicate that annealing within a 400-900° C range leads to an increase in hardness due to the strain hardening and ordering processes; the residual stresses developing as a result of this are unlikely to be the source of cracking due to their low magnitude. An increase the heating rate alters the course of these processes, making it possible to conclude that the decay processes can be partially suppressed and the ordering processes can be shifted to the area of higher temperatures. It is noted that correct selection of the annealing temperature makes it possible to increase the total alloy reduction to 70 percent. Figures 3; references 6.

Statistical Methods of Studying Effect of Process Factors on Alloyed Steel Losses During Heating

937D0030H Moscow IZVESTIYA VYSSHIKH UCHEBNYKH ZAVEDENIY: CHERNAYA METALLURGIYA in Russian No 3, Mar 92 pp 73-75

[Article by V.Ye. Nikolskiy, Dnepropetrovsk Chemical Engineering Institute; UDC 621.036:621.783.23]

[Abstract] High metal losses due to the surface layer oxidation and decarburization prompted an attempt to establish the effect of such hitherto poorly known factors as the combustion products' temperature and the rate of flow of these about the metal surface at various gaseous atmosphere compositions on the decarburization process. The computation analysis is carried out on a YeS-1022 Unified Series computer using the following variables: the heat flux, flow velocity, flow segment length, and metal surface temperature. The carbon concentration gradient in the surface layer under various combustion product compositions and flow velocities is plotted, and the experimental design method is used in order to reduce the number of tests using the following factors: the furnace temperature, process duration, and gaseous atmosphere composition. Two chamber furnaces are used in the experiment: one equipped with a Giproaviaprom burner and one with a GPPs-4 arch burner using a natural gas and air fuel. Regression equations are derived for calculating the metal burning loss and establishing the relation between the above factors and the total metal loss to oxidation. An analysis shows that a decrease in the combustion product layer temperature near the metal and flow velocity decreases the diffusion flow of carbon in the boundary layer and helps to reduce the steel decarburization. The use of plane-parallel burners lowers oxidation and decarburization compared to traditional burners due to the combustion product uniformity and elimination of incomplete combustion product contact with the metal. Figures 1; references 7.

Carbide Coatings on Steel, Cast Iron Parts

927D0250C Kiev AVTOMATICHESKAYA SVARKA in Russian No 3, Mar 92 pp 44-45

[Article by Yu. S. Borisov, Ye. N. Shavlovskiy, and N. I. Kaporik, Institute of Electric Welding, Ukrainian Academy of Sciences; UDC 621.78.063.4:[661.876.621+661.888.1.621]: [669.14+669.13]]

[Abstract] The Institute of Electric Welding has developed a process for coating steel and cast iron parts with vanadium and chromium carbides to make them resistant to wear and corrosion. With vanadium carbide coatings, the thickness of the hardening layer on parts made of various steels and cast iron is 5-20 micrometers, and with chromium carbide coatings the thickness is 5-40 micrometers. The microhardness in both cases is 26,000-29,000 N/mm^2 and 1,500-1,600 N/mm^2, respectively. Vanadium carbide coatings withstand temperatures up to 400° C, and chromium carbide coatings withstand temperatures up to 850° C.

The coating process is a final operation; the part does not require machining. The process consists of heating the part in a molten salt that has carbide-forming elements added to it. The process temperature is 800-1100° C with exposure time of 0.5-3.0 hours. The materials required are inexpensive and readily available, and they can be used repeatedly. The process is conducted at atmospheric pressure and does not require shielding media. Heat treatment of the coated products is done immediately after they are removed from the saturating bath. The process is intended for hardening machine parts which operate in conditions of friction and wear, high temperatures, and corrosion.

Results of industrial trials of the coatings on various types of parts are noted.

Corrosion Resistance, Gas-Abrasive Wear of Plasma-Applied Coatings

927D0250D Kiev AVTOMATICHESKAYA SVARKA in Russian No 3, Mar 92 pp 45-48

[Article by V. F. Golnik, A. L. Gaydarenko, Z. G. Ipatova and Yu. K. Vysotskiy, Institute of Electric Welding, Ukrainian Academy of Sciences; UDC [621.793.72:533.9]:620.193]

[Abstract] Plasma-applied coatings of iron and nickel-base alloys were investigated for their electrochemical behavior and corrosion resistance in hydrochloric solutions of various concentrations, their gas-abrasive wear at different angles of attack of the abrasive, and their resistance to wear in conditions of sliding friction at a constant sliding rate under different loads. A coating of the system Fe-Cr-Mo-B was found to have the highest corrosion resistance. An amorphous microcrystalline structure forms when this coating is applied. Wear tests in conditions of gas-abrasive wear showed that at all angles of attack of the abrasive, this characteristic is highest in coatings made of the powder PG-SR-3 after fusion, and it is lowest in coatings of Fe-Cr-Mo-B, which is due to the high porosity of this coating.

Ceramic Coatings for Protecting Structural Elements of Heating Installations

927D0250E Kiev AVTOMATICHESKAYA SVARKA in Russian No 3, Mar 92 pp 48-50

[Article by St. Morel and Sl. Morel, Czestochowa Polytechnical Institute, Poland; UDC [621.793.72:533.9]: [669.15.693:66.042.88]

[Abstract] It is demonstrated that the temperature of heat-radiated walls of heat exchangers can be lowered by applying ceramic coatings to them. Heat conduction and wear resistance of coatings applied to structural elements of heating installations are examined. A measurement/test bed and the testing methods for this are described, and an analysis is made of the effect of the coating type on the amount of heat drawn off from a torch by water flowing through model heat exchangers. It was found that zirconium oxide coatings have the highest capability of limiting removal of heat by cooling elements of heating installations.

Testing Coat Properties for Forecasting Turbine Blade Service Life

937D0026H Kiev PROBLEMY SPETSIALNOY ELEKTROMETALLURGII in Russian No 2 (30), Apr-Jun 92 pp 43-49

[Article by L.B. Getsov, I.S. Malashenko, A.I. Rybnikov, L.G. Padva, Yu.B. Shneyerson, Proletarskiy zavod Production Association, St. Petersburg, Electric Welding Institute imeni Ye.O. Paton at the Ukrainian Academy of Sciences, Kiev, and Scientific Production Association at the Central Boiler and Turbine Institute imeni I.I. Polzunov; UDC 669.187.526.001.2]

[Abstract] The task of predicting the service life of turbine blades with condensed high-temperature coats by theoretically determining the coat material characteristics on the basis of a data bank accumulated from tests of vacuum deposited condensate coats with various compositions is addressed; it is noted that service life prediction requires data on the behavior of the modulus of elasticity, thermal coefficient of linear expansion (TKLR), the dependence steady state creep rate on stress, the straining diagram, and resistance to thermal fatigue as a function of the temperature conditions within a broad temperature range. The dependence of the thermal coefficient of linear expansion on the Ni and Al concentration at various temperatures and on temperature at various component concentrations, the straining resistance of various condensates at 800° C, and creep resistance of condensates at 800° C are plotted. The thermal cycling endurance of electron beam and other coats deposited on Ni-based superalloys is summarized. It is stressed that longevity analyses of superalloy turbine blade coats call for joint efforts of many researchers in accumulating sufficient databases. The proximity of experimental and theoretical data attests to the adequacy of the analytical estimates of the physical and mechanical characteristics which cannot be easily measured. Figures 4; tables 1; references 14: 12 Russian, 2 Western.

Effect of H_2O_2 on Anodic Dissolution and Corrosion of Homogeneous Ag-Zn System Alloys

937D0032A Moscow ZASHCHITA METALLOV in Russian Vol 28 No 5, Sep-Oct 92 pp 725-729

[Article by N.N. Letichevskaya, V.Yu. Kondrashin, I.K. Marshakov, Voronezh State University; UDC 541.138.2]

[Abstract] The lack of experimental data on the reduction of oxygen-bearing oxidizers on metal electrodes and its positive effect on anodic dissolution of the metal itself prompted a study of the effect of hydrogen peroxide on the anodic dissolution and corrosion of homogeneous Ag-Zn alloys. To this end, α-, β-, γ-, and ε-phases and pure Ag and Zn are examined experimentally under potentiostatic conditions on a spinning disc electrode at 12 RPM in a deaerated solution of 95 mM K_2SO_4 + 5 mM H_2SO_4 (i.e., the background solution) and in the same medium with an H_2O_2 addition to a 0.01 M level. The dependence of the Zn^{2+} concentration on the anodic dissolution duration of the γ-phase in two types of solutions, the relative enhancement of the anodic dissolution of Ag and Zn phases with hydrogen peroxide additions, and the anode and cathode polarization curves of self-dissolution of the Ag-Zn system are plotted. The anodic dissolution current of Zn, Ag, and Ag- and Zn-phases under varying conditions are summarized. The findings confirm that during the initial selective Zn dissolution on the α-phase, an Ag-enriched zone is formed. Alloys with a high Zn content with a proclivity to selective dissolution with a phase transformation on the surface behave as pure Zn in relation to H_2O_2, thus making it possible to speculate that the Zn concentration on the α-phase is virtually nil while on the surface on the β-, γ-, and ε-phases it is noticeable to such a degree that its ionization has a dominant effect on the total anodic process rate. In the presence of oxidizers ensuring a high cathode process rate, a sharp acceleration of anodic dissolution leads to a jump-like increase in the corrosion resistance of alloys due to the formation of adsorbed OH^- ions during the transition from the α- to β-structure. Figures 3; tables 1; references 9.

Formation of Anode Films on Tantalum in $LiClO_4$-Aprotonic Solvent Systems

937D0032B Moscow ZASHCHITA METALLOV in Russian Vol 28 No 5, Sep-Oct 92 pp 730-734

[Article by V.P. Grigoryev, O.N. Nechayeva, V.E. Gorelik, Rostov State University and Scientific Research Institute of Physical and Organic Chemistry at the Rostov State University; UDC 620.193.47]

[Abstract] The scarcity of data on the anodic oxidation of tantalum in aqueous electrolyte solutions prompted a study of the formation kinetics of anodic oxide films on the Ta surface in aprotonic media and the effect of the solvent origin on this process. The study is carried out in a 0.1 M solution of $LiClO_4$ in the following aprotonic solvents: acetonitrile (AN), propylene carbonate (PK), acetone (Ats), dimethyl formamide (DMFA), and dimethyl sulfoxide (DMSO). The oxide film development kinetics are examined by potentiostatic chronoamperometry at a potential corresponding to different segments of the anode polarization curves. The potentiodynamic tantalum anode polarization curves in various solvents, the dependence of the current density i on $1/\tau$, the dependence of $\lg i$ on $1/\tau$, and the dependence of the $\lg(1/\tau_{cr})$ on the slopes, the quantity of electricity, and solvent's donor number are plotted. The critical time at which the logarithmic oxide growth law changes to parabolic decreases with an increase in the donor number DN. Linear correlations between the DN and the film growth process parameters attests to the donor-acceptor interaction of the solvent molecules with the metal surface. The lack of linear correlation between the growth rate and dielectric permittivity of the solvent points toward an insignificant role of the medium's electrostatic properties in the film development. The film spread rate on the metal surface increases with the DN while ionic conduction decreases. Under growth by a parabolic law, the film growth rate is limited by diffusion of metal atoms and does not depend on the nature of the solvent. Figures 4; tables 2; references 18: 14 Russian, 4 Western.

Study of Surface Composition and Corrosion Resistance of Welded Joints From Zr + 1 Percent Nb Alloy

937D0032C Moscow ZASHCHITA METALLOV in Russian Vol 28 No 5, Sep-Oct 92 pp 735-743

[Article by E.Kh. Yenikeyev, A.K. Feoktistov, L.N. Shchavelev, B.B. Butylkin, Physical Chemistry Institute at Russia's Academy of Sciences; UDC 620.193: 621.791.053:546.831]

[Abstract] The effect of niobium additions on the protective corrosion film on zirconium and the kinetics of the zirconium alloy oxidation processes are discussed; the surface properties of welded joints and heat affected area of a Zr+1 percent Nb alloy made by argon arc welding as well as the corrosion resistance of the weld and heat affected zone (ZTV) metal are examined. In so doing, the N_2, O_2, and H_2 concentration in argon is manipulated within a 5 x 10^{-5} to 1 x 10^{-1} percent. Corrosion tests are carried out for 120 hours at a 350° temperature and 168 atm pressure in autoclaves in a steam and water medium using samples cut in the shape of chutes. The surface composition is determined by mass spectrometry of secondary ions with a liquid Ga source with a submicrometer resolution and by X-ray electron spectroscopy with a MgK anode. The mass spectra of secondary ions and X-ray electron spectra of the alloy surface are plotted. An analysis confirms an electron density transfer from Zr atoms to impurity atoms which are segregated on the weld surface. Zr is a transition metal whose metallic bond is formed by the overlapping spherical s^2 Zr atom shells. Since Zr is at the start of group IV in the periodic table, the d-zone is relatively poorly populated, so the acceptor impurity

segregation (O or N) pushes some levels responsible for the Zr-Zr bond to a higher energy region which may partially weaken the Zr-Zr bonds and increase the oxidation rate at the stage controlled by the surface reaction. The issue of the welding medium is dominant for crucial corrosion resistant parts, so the impurity concentration should not exceed GOST levels since the corrosion rate is proportionate to the impurity concentration in the shielding argon welding gas. Figures 3; tables 1; references 15: 6 Russian, 9 Western.

Correlation of Composition and Protection Effectiveness of Conversion Chromate Coats on Mg

937D0032D Moscow ZASHCHITA METALLOV in Russian Vol 28 No 5, Sep-Oct 92 pp 744-749

[Article by A.Yu. Simaranov, A.I. Marshakov, Yu.N. Mikhaylovskiy, Physical Chemistry Institute at Russia's Academy of Sciences; UDC 620.197.6]

[Abstract] The relationship between the protective properties of conversion chromate coats (KKhP) and their thickness and composition, particularly the ratio of Mg(II) and Cr(III) hydroxides, is discussed, and an attempt is made to identify the correlation between the composition of a dense conversion chromate coat on magnesium and its protection efficiency. To this end, the protection effectiveness is determined by measuring the volume of hydrogen liberated as a result of corrosion of samples during five hours in a 0.5 percent Na Cl-V_{H_2} solution. The conversion chromate coat metal formation rate is measured by comparing the initial sample mass to the mass after the coat is applied and removed. The behavior of the mass of alkali-insoluble chromate coat component formed at various concentrations and the dependence of the hydrogen volume liberated during the corrosion tests on the ratio of the chromium and magnesium hydroxide formation rates z are plotted. The study shows that an increase in the chromate concentration in the electrolyte leads to an increase in the $Cr(OH)_3$ content in the dense hydroxide layer and that the chromate coat's protective properties are due to the presence of this hydroxide as a result of a change in the sign of the surface hydroxide layer potential on the metal. An addition of Zn cations to the solution substantially increases the coat effectiveness. It is reiterated that the coat consists of a dense Mg(II) and Cr(III) hydroxide layer on the base with a porous $Cr(OH)_3$ layer formed by selective dissolution of magnesium hydroxide from the dense layer. Figures 2; tables 2; references 8: 6 Russian, 2 Western.

Comparative Characteristics of Anodic Behavior of Steel 08kp in Zinc Sulfate, Nitrate, and Monophosphate Solutions Doped With Sodium Nitrite

937D0032E Moscow ZASHCHITA METALLOV in Russian Vol 28 No 5, Sep-Oct 92 pp 756-759

[Article by V.A. Chumayevskiy, V.V. Selevin, Kristall Scientific Production Association and Buy Chemical Plant; UDC 621.794]

[Abstract] The dependence of the state of the metal surface and reaction rates on it on the initial surface condition at the moment of contact with the solution during chemical phosphatizing of steel is discussed, and the anodic behavior of steel 08kp in a number of model solutions containing zinc sulfate, nitrate, and monophosphate ions with and without $NaNO_2$ additions is examined. The anode polarization and schematic curves of steel 08kp at a 55°C temperature in various solutions are plotted. The study is confined to the first 5-10 seconds after contact which determine the growth, thickness, and quality of the phosphate film. An analysis of the steel surface behavior points to two competing mechanisms: surface passivation with nitrates and nitrites and their participation in the elementary event of the iron ionization reaction. The nitrite ions have a greater passivating effect than the nitrate ions which is evident in the increase in Tafel's constant. The need for further studies of the complex interrelation of the cathode and anode reactions occurring on the surface is stressed. Figures 4; references 16: 14 Russian, 2 Western.

Pitting On Bi in Aqueous Solutions

937D0032F Moscow ZASHCHITA METALLOV in Russian Vol 28 No 5, Sep-Oct 92 pp 768-773

[Article by Yu.I. Kuznetsov, S.Yu. Reshetnikov, Physical Chemistry Institute at Russia's Academy of Sciences; UDC 620.193.01]

[Abstract] The convenience of bismuth electrodes as a model for studying local anodic depassivation prompted an investigation into the promotion and inhibition of local bismuth depassivation in aqueous solutions with various pH and anodic compositions and the effect of adsorption-type inhibitors on the local depassivation process. The study is carried out using cylindrical 98 percent pure Bi samples in naturally aerated borate solutions with pH = 6.0 -10.0 containing sodium salts as activators and sodium phenylanthranylate (FAN) as an inhibitor. The effects of the solution anion origin and concentration on bismuth's pitting potential in the buffer is examined, and the anode polarization curves of Bi in borate buffers with and without activators at various pH, the dependence of the effective pitting overvoltage on the activator activity in the solution at pH = 7.4 and 6.5, and the dependence of the pitting potential on the chloride ion activator and FAN concentration are plotted. An analysis of the curves shows that the pitting overvoltage on Bi decreases linearly with an increase in the cation activity and water repellent property while the latter has a decisive effect on the pitting potential in neutral activator solutions which can be best expressed by a single parameter equation. The initial stages of Bi depassivation can be better inhibited by using water repellent anions, such as FAN, especially at concentrations exceeding 10 mM. It is noted that there is no pitting in solutions containing carboxylate ions at an alkyl number of >5. Figures 3; references 11: 10 Russian, 1 Western.

Effect of Soil on Spectroscopic Characteristics of St3 Surface Under Cathodic Protection Conditions

937D0032G Moscow ZASHCHITA METALLOV in Russian Vol 28 No 5, Sep-Oct 92 pp 780-785

[Article by Ye.G. Kuznetsova, R.M. Lazorenko-Manevich, L.A. Sokolova, L.V. Remezkova, Public Service Utilities Academy imeni K.D. Pamfilov and Scientific Research Physical-Chemical Institute imeni L.Ya. Karpov; UDC 620.193.01.197.5]

[Abstract] The effect of the soil conditions, e.g., type, moisture content, and soil electrolyte composition, on the kinetics and character of corrosion failure of carbon steel in soil is discussed, and the importance of electric reflection (EO) spectroscopy for determining the state of the steel surface and the presence of adsorbed compounds is noted. Electric reflection spectra of steel St3 after corrosion in moistened sand and clay are analyzed in order to assess the likely causes of the differences observed in the corrosion behavior of steel in these soils. To this end, the experiment is carried out in a 0.1 M NaOH solution at a high pH. The role of the oxide film in the St3 behavior in various soils is estimated by the electric reflection spectra in a 0.03 M NaCl+0.015 M Na_2SO_4 solution at pH = 13 with EDTA additions. All spectra are recorded at a 30 Hz potential modulation frequency and a 30 mV amplitude. The electrodes are exposed for 60 days without cathodic protection. The Re and Im spectra of two electrodes before and after cathodic reduction and with and without EDTA (ethylenediaminetetracetic acid) are plotted. An analysis of the samples and EO spectra curves shows that the steel surface after exposure to moist clay is less nonuniform in relation to water adsorption than the initial sample surface or the surface of samples exposed to moist sand. The change in the water adsorption center distribution is attributed to strong adsorption of the surface active components on clay soil which leads to an increase in the corrosion resistance. After extended cathode polarization, the surface active component contained in clay is desorbed and the spectra assume their initial shape; the conclusion is drawn that the EO spectra shape is not affected by the oxide film but is determined by the surface active component adsorption. It is noted that available data are insufficient for speculating about the origin of this component; judging from the energy of available charge transport bands (PPZ), the St3 surface after contact with soil is less active than the initial St3 surface. Figures 3; references 8: 6 Russian, 2 Western.

On Taking Into Account Conical Shape of Holes in Model Electrode Coat for Monitoring Cathodic Protection of Underground Pipelines

937D0032H Moscow ZASHCHITA METALLOV in Russian Vol 28 No 5, Sep-Oct 92 pp 786-792

[Article by L.I. Freyman, Public Service Utilities Academy imeni K.D. Pamfilov; UDC 620.197.5.198]

[Abstract] The issue of selecting the shape of the model electrode (i.e., a potential transducer) for monitoring the cathodic protection effectiveness of underground steel pipelines pursuant to GOST 0.602-89 is addressed, and an attempt is made to demonstrate theoretically that the cathodic protection monitoring efficiency correctness depends on the slope of the channel walls in the insulation at least as much as it does on the size which determines the model surface area or insulation thickness. The cross sectional view of the through defect (a hole) in the insulating coat with straight and sloping channel walls, the dependence of the simulated defect diameter on the model channel wall slope, and the dependence of the maximum and minimum permissible insulation defect channel wall slopes, and the angle range on the pipe coat thickness are plotted. The boundary values of the simulated insulation defect diameter at a 30 mm model diameter at the minimum and maximum pipeline coat thickness are summarized for two sets of models each having four standard sizes. The findings show that for correct monitoring of the cathodic corrosion protection of underground steel pipelines with the help of a model disc electrode, the selection of the insulation thickness and channel wall slopes in the insulation is crucial. The possibility of theoretically calculating the model parameters as a function of the specific practical conditions is demonstrated. Figures 4; tables 1; references 5.

Programmed Electrodeposition of Sn-Cu Microlayered Alloy

937D0032I Moscow ZASHCHITA METALLOV in Russian Vol 28 No 5, Sep-Oct 92 pp 816-819

[Article by N.A. Kostin, V.M. Zamurnikov, Dnepropetrovsk Railroad Engineers Institute; UDC 621.359.539.2:541.138]

[Abstract] The advantages of multilayer electrolytically deposited coats prompted an attempt to develop a programmed deposition method by pulsed current from a sulfate electrolyte containing 30 g/l of Sn, 10, 14, or 21 g/l of Cu, 100 g/l of H_2SO_4, and 2.5 g/l of OP-10 at an 18-25°C temperature using tin and stainless steel anodes on a copper base. The polarization measurements are taken in pulsed modes by an oscilloscope; the phase composition of the coats is studied by a DRON-2 X-ray diffractometer in Cu-radiation with a Ni-filter. The deposit microhardness is measured by a PMT-3 instrument at a 0.2 N indentor load. The wear resistance is measured in a Kh4-B friction tester. The qualitative polarizing programmed current and cathode potential diagrams, X-ray diffraction patterns of the Cu and Sn-Cu alloy layers electrodeposited by programmed pulse current, and the dependence of the Sn concentration in the Sn-Cu alloy on the mean programmed current pulse density are plotted. The method can be used to deposit layers of different metals or from the same metal but with a different structure and properties. Such layered composite deposits may contain layers with deliberately "poor" properties for individual uses, but when

they alternate with other layers, they improve such properties as wear and corrosion resistance. By precipitating microlayers with a different thickness and structure one can impart the necessary functional properties in the coat. Figures 3; references 4.

Inhibiting Effect of Benzimidazole and Benzotriazole on Corrosion of Steel 12Kh18N10T in H_2SO_4

937D0032J Moscow ZASHCHITA METALLOV in Russian Vol 28 No 5, Sep-Oct 92 pp 842-845

[Article by G.O. Tatarchenko, N.F. Tyupalo, V.S. Kuzub (deceased), A.B. Sukhomlinov, B.A. Gru, Rubezhansk Branch of the Dnepropetrovsk Chemical Engineering Institute and State Scientific Research and Design Methanol Institute; UDC 547.765.5:620.197.3]

[Abstract] The inhibiting action of various concentrations of benzimidazole (BIA) and benzotriazole (BTA) in sulfuric acid on the corrosion of steel 12Kh18N10T is studied by gravimetric, polarization, and electrocapillary measurements as well as by quantum chemical using the ChPDP/3 method. To this end, clean, degreased, and weighed samples are activated in concentrated HCl for one minute and washed in distilled water prior to 100 hour corrosion tests. The electrocapillary Hg curves in deaerated solutions with various compositions and polarization curves of steel 12Kh18N10T in aerated solutions with various compositions are plotted, and the quantum chemical parameters, e.g., the dipole moment, ionization constant, and π- and π + σ-charges, are summarized. An analysis of the findings indicates that under cathodic protection conditions, a benzimidazole addition is more effective than benzotriazole, yet at a zero charge potential, the opposite is true. In a 20 percent sulfuric acid solution, the different orientation of the benzimidazole and benzotriazole molecules on the surface determines the difference in the level population limits. In a pure 20 percent solution of H_2SO_4, the corrosion rate is 3.5 g per square meter per hour but with benzimidazole and benzotriazole additions it drops to 2.5 and 0.008, which corresponds to a protection degree of 21.25 and 99.44 percent; at a 5 percent BIA concentration, the corrosion rate is 0.006 g/m^2 per hour. Figures 3; tables 1; references 7: 5 Russian, 2 Western.

Carbonic Acid Hydrazides as Steel Corrosion Inhibitors

937D0032K Moscow ZASHCHITA METALLOV in Russian Vol 28 No 5, Sep-Oct 92 pp 845-848

[Article by A.V. Radushev, A.B. Shein, R.G. Aitov, V.Yu. Gusev, N.F. Petina, G.I. Popov, N.B. Tarasova, Engineering Chemistry Institute at the Urals Branch of Russia's Academy of Sciences, Perm State University, and Perm Scientific Research and Design Petroleum Institute; UDC 620.197.3]

[Abstract] The ability of fatty carbonic acid hydrazides (GZhK) with a C_7-C_{12} radical and natural naphthenic acids (GNK) to inhibit the corrosion of steel on hydrochloric, hydrosulfuric, and real oil field water is examined. Since hydrazides of fatty carbonic acids are both scarce and expensive, hydrazides of synthetic fatty acids (GZhK) are used in the study. To this end, both hydrazides of synthetic fatty and natural naphthenic acids are synthesized from methyl ethers of the corresponding carbonic acids and hydrazinehydrate. Samples of steel 08kp are cleaned with a fine abrasive paper, degreased in alcohol, weighed, and placed in acidic solutions with and without the hydrazides. Formulae are derived for calculating the steel corrosion and the protective action of the hydrazides whose inhibiting effect is determined by the gravimetric method in a Gardner column. The rate of acid corrosion of steel 45 and the protective action of the hydrazine additions, the corrosion rate in a model waste water without hydrogen sulfide and the protective action of hydrazides, and the corrosion rate and protective action of hydrazides in model waste water with hydrogen sulfide and real oil field water are summarized. In 0.1 n HCl, the protective action of GZhK is observed at a C_7-C_8 radical length and reaches 82-96 percent at a 9-12 radical length. As the chain length increases, the GZhK solubility decreases. GNKs are the most effective in model waste waters with and without H_2S: the protective action Z reaches 91-97 percent at a 75-100 mg/l addition. GNKs effect in oil field water in Perm reaches 90-97 percent at a 100 mg/l addition. Tables 4; references 3.

Effect of Oxidizers on Corroding Ti-Electrode Impedance

937D0032L Moscow ZASHCHITA METALLOV in Russian Vol 28 No 5, Sep-Oct 92 pp 856-858

[Article by Kh.G. Kochukbayev, V.I. Kichigin, Natural Sciences Institute at the Perm State University; UDC 620.197.3]

[Abstract] It is speculated that inhibitors may participate in the development of an oxide film on electrodes, particularly titanium electrodes in oxidizing media. Consequently, the corroding Ti-electrode impedance and the effect of the oxide film on this impedance are examined in pure acid solutions and in the presence of a number of inorganic and organic oxidizers; to this end, cylindrical VT1-00 titanium samples are embedded in teflon, the end surface is mechanically polished, degreased, and activated in sulfuric acid or placed in a cell with a surface oxide formed in the air. The impedance is measured two-three hours and 24 hours after immersing the electrode in the solution at a 10^5-10^{-3} Hz. The solutions are prepared from distilled acids and bidistillate using aerated or deaerated hydrogen at a 295K temperature. The locus curves of the corroding Ti-electrode impedance in various solutions and the dependence of the polarization resistance logarithm and high-frequency capacitance of activated and nonactivated Ti on the corrosion potential in the presence of oxidizers are plotted. The study shows that the solution aeration with hydrogen does not significantly alter the behavior patterns. Titanium's polarization resistance in an acid with an oxidizer depends on the sample preparation method; given the same preparation, the curves are almost identical for most acids and oxidizers. No specific inhibitor interaction with the surface oxide is detected. Figures 2; references 8: 2 Russian, 6 Western.

An Expert System To Control a Blast-Furnace Smelting Process

937D0003A Moscow STAL in Russian
No 7, Jul 92 pp 15-18

[Article by M.M. Frenkel, Yu.V. Fedulov, O.A. Belova, V.A. Krasnobayev, and T.M. Yakhno, Chermetavtomatika Scientific Production Association, Magnitogorsk Metallurgy Combine, and Computer Center, Siberian Department, Russian Academy of Sciences; UDC 669.162]

[Abstract] The main problems in controlling the course of a blast-furnace smelting process are the indeterminacy of the manner in which the process will unfold and the fact that the equipment will react differently depending on the composition and properties of the given charge. The authors of the study reported herein worked to develop an expert system to control blast-furnace smelting processes in view of the inherent indeterminacy of the process. An expert system to assist blast furnace operators was developed by the Chermetavtomatika Scientific Production Association in collaboration with the Intex GNF [not further identified], the Computer Center of the Siberian Department of the Russian Academy of Sciences, the Control Problems Institute, and the Magnitogorsk Metallurgy Combine. The new expert system, which was tested with the No. 8 furnace at the Magnitogorsk Metallurgy Combine, included the following components: knowledge accumulation (formalization of the knowledge possessed by expert metallurgists and the creation of a knowledge base); process diagnostics (the ability to detect anomalous states, i.e., disruptions, in the course of the blast-furnace smelting process); technology optimization (the ability to determine optimal control strategies and select process parameter values); a simulator (means for training and testing the knowledge of metallurgists); a data base manager (a system to perform all operations involving the information present in the system); and an automated reference information system (a system containing reference materials, training materials, and a glossary that are all designed to assist metallurgists in making professional calculations). The expert system is designed for installation on an IBM PC AT-type personal computer with an EGA/VGA video adapter, at least 640 K of working memory, at least 25 Mbytes of disk space (about 12 Mbytes is required for standard software and more than 11 Mbytes is required for software unique to the expert system). The new expert system operates with the MS DOS operating system and may be used by different users with open and hidden passwords, names, or groups. All of the expert system's original software, shells, and knowledge bases are protected against unauthorized corrections, study, or copying. The test at the Magnitogorsk Metallurgy Combine was designed to address a number of problems ranging from determining the simplicity of communicating with the expert system in natural language (i.e., in Russian) to determining the appropriateness of the conclusions and recommendations issued by the system on the basis of the information contained in it. The tests confirmed the new expert system's effectiveness in breaking down the language barrier that metallurgists encounter when attempting to access the intellectual capabilities of a computer. Figures 2; references 6: Russian.

The Effect of a Metal Melt's Structure and Properties on the Quality of Castings

937D0003B Moscow STAL in Russian
No 7, Jul 92 pp 21-28

[Article by E.V. Kolotukhin, B.A. Baum, Ye.A. Kuleshova, V.N. Larionov, Ye.Ye. Tretyakova, and G.V. Tyagunov, Ural Polytechnic Institute and All-Union Aviation Materials Scientific Research Institute; UDC 669.245:620.186.82]

[Abstract] A study examined the effect that the structure and properties of the starting metal melt have on the quality of castings produced from nickel-and-chromium-based refractory alloys with small amounts of tungsten added to them. Seven melts were studied in all. The experiments performed established that the temperature of the onset of intensive structural transformations of the individual melts studied depends on their carbon content and on their total concentration of γ'-forming elements (Al, Ti, Nb, Hf, and Ta). The study findings enabled the researchers to propose a physical picture of the structure of molten refractory alloys that is a further development of the quasi-chemical version of the model of the microinhomogeneous structure of microcomponent melts. The model is based on the idea of the existence of an interaction between Ni_3Al-type microformations that takes place in metal above the liquidus point and that leads to the formation of a bulk structure. The destruction of this structure leads to the formation of polyclusters of particles of refractory compounds measuring 1 to 10 nm in size and surrounded by an Ni_3Al-type microformation. The researchers also examined the effect of the technique of high-temperature melt treatment on the micro- and macrostructure of castings made of the said melts and on the quality of components made of refractory alloys. High-temperature melt treatment proved to improve the structure of castings and the performance characteristics of products made from them, as well as to reduce the amount of defective products produced. The main benefit of high-temperature melt treatment was that it reduced the amount of nitrides, carbonitrides, oxides, and scabs in the metal produced. Refractory alloys subjected to high-temperature melt treatment were found to be characterized by increased castability. After comparing the effects of several different methods of treating metal after high-temperature melt treatment, the researchers concluded that post-high-temperature melt treatment regimens must be tailored to the specific melt under consideration. One of the melts tested required four hours of homogenization at 1,180° C followed by 16 hours of aging at 900° C (at which point a secondary γ'-phase appears in the structure of the metal) in order to produce an alloy with better mechanical characteristics than those of series-produced metal. Monocrystalline samples of two other melts with a more finely dispersed

γ'-phase and more evenly distributed dendrite cell did not, on the other hand, require standard heat treatment, i.e., homogenization followed by aging, and may be dispensed with. Instead, the two melts only required a two-stage aging process. The researchers called for further research to optimize all stages of the process of producing components from metal that has been subjected to high-temperature melt treatment. Figures 8; references 11: Russian.

The Efficiency of Casting Hollow Ingots on Continuous Billet Casting Machines

937D0003C Moscow STAL in Russian No 7, Jul 92 pp 36-37

[Article by I.K. Marchenko, M.Ya. Brovman, V.V. Anikeyev, and V.A. Dubonosov, Machine Building Scientific Research, Design and Technology Institute Production Association; UDC 621.746]

[Abstract] The Machine Building Scientific Research, Design and Technology Institute Production Association [NPO NIIPTmash] has assimilated a semicontinuous process of casting hollow ingots with outer diameters of 270 and 500 mm and thicknesses of 50 and 135 mm from carbon and alloy steels. The metal is fed into the annular gap between a continuous casting mold and mandrel by means of a casting cup with two to four channels along the continuous casting mold's perimeter. The mandrel has a steel casing with a copper outer shell mounted on a thread in its upper part. The mandrel's outer surface has a conicity of 1:50 for ingots with an outer diameter of 270 mm and 1:90 (on the upper section of the mandrel) and 1:180 (on the lower section) for ingots with an outer diameter of 500 mm. The mandrel swings together with the continuous casting mold. The inner shells of the cast ingots are cooled with water that is sprayed in through nozzles under the mandrel. Ingots with outer diameters of 270 and 500 mm move along at rates of 0.14-0.16 and 0.08-0.12 m/min. A slag mixture containing Portland cement, fluorspar, nepheline concentrate, silicate fragments, and amorphous graphite is used to protect the heel of the metal from secondary oxidation and cooling. Tests of the new continuous casting technique and machine have confirmed that it produces ingots free of surface flaws and with a sufficiently dense microstructure and uniform chemical composition. The distribution of oxides and sulfides in the end zones of the hollow ingots produced is essentially even, as are the distributions of oxygen and nitrogen along the height and cross sections of the ingots. The new technique was used to produce a batch of hollow ingots that were in turn used to manufacture a large test batch of cylindrical dies. The new technique made it possible to produce 15 to 18 percent more nondefective dies than can usually be produced from continuous ingots. Figure 1.

Alloying Steel With Vanadium By Using Ash Wastes From GRES

937D0003D Moscow STAL in Russian No 7, Jul 92 pp 37-40

[Article by A.Ye. Sochnev, Yu.G. Yaroslavtsev, V.A. Kurganov, L.V. Agranonik, and Yu.M. Nerovnyy, Don Ferrous Metallurgy Scientific Research Institute; UDC 669.18.046.516.2:669.046.546.2]

[Abstract] According to estimates the boiler furnaces at state regional electric power stations [GRES] currently burn about 100 million tons of sour petroleum residue. This residue contains 10,000 tons of vanadium and 2,000 tons of nickel. Ninety percent of the vanadium is deposited on the boilers' heating surfaces in the form of ash and slag. The amount of ash currently collected at GRES is sufficient to produce 200,000 to 400,000 tons of steel per year. A portion of the vanadium ash formed at GRES is currently used to produce ferrovanadium that is in turn used in the steel-alloying process. The losses of vanadium in the process run as high as 50 percent, however. In view of these facts, the authors of the study reported herein worked to develop a method of making direct use of the ash wastes from GRES when alloying steel with vanadium. Specialists at the Donetsk Metallurgy Plant developed and tested (under laboratory conditions) a mixture for alloying steel with vanadium in a ladle. Part of the sulfur is removed as the mixture is burned. The remaining sulfur is absorbed by the calcium oxide of the slag formed during the combustion process. To prevent possible resulfurization, the refined slag prepared in the furnace at the end of the melting is released to the ladle, after which the metal is released. Tests established that between 90 and 98 percent of the vanadium is extracted when the steel is alloyed in the ladle. Because alloying steel directly in the ladle requires additional equipment for preparing the mixtures and the construction of a unit to produce a slag-metal foundry alloy in the ladle and removing and cleaning the resultant gases, a simpler procedure was developed to alloy steel with vanadium directly in an electric furnace. When steel is alloyed directly in a furnace, the degree of vanadium extraction is determined by how completely it is reduced and ranges from 70 to 90 percent. Tests comparing the quality of the metal produced by the new direct alloying process with that of control specimens confirmed that the new vanadium alloying process results in steel possessing mechanical properties that are on a par with those of conventionally alloyed steels and that meet the requirements specified in existing standards. Both the test and control specimens contained virtually identical amounts of impurities. Tables 2; references 2: Russian.

On Correlation Between Ultimate Specific Strain Energy and Steel Hardness

937D0029C Moscow IZVESTIYA VYSSHIKH UCHEBNYKH ZAVEDENIY: CHERNAYA METALLURGIYA in Russian No 4, Apr 92 pp 41-43

[Article by V.A. Skudnov, A.N. Severyukhin, Gorkiy Polytechnic Institute; UDC 669.046:539.4.014.1]

[Abstract] Interest in the energy criteria of fracture in the study of metal failure and the lack of data on the correlation of the strain energy, hardness, ultimate strength, yield, and toughness prompted an investigation into the dependence of the ultimate specific strain energy on the structural energy state index, which is proportionate to hardness, of ten

structural classes of steel. A formula for calculating the structural state index is derived and the ultimate strain energy is calculated on the basis of known data. The dependence of the ultimate specific strain energy on the index is tabulated for 40 steels belonging to the above ten categories; in addition, the dependence of the ultimate specific strain energy on the structural energy state index of carbon, ferritic, martensitic-ferritic, pearlitic, martensitic, austenitic-ferritic, austenitic, austenitic-martensitic, maraging, and pearlitic-martensitic steels is plotted. The findings demonstrate that the correlation between the ultimate specific strain energy and hardness does not follow a predictable pattern under diverse effects on the iron and steel structure created by changing the chemical composition, structure, and heat treatment; rather, the domains of states of various classes of steel fall within certain energy and hardness ranges. This makes it possible to assert that such serviceability parameters as wear resistance of each class of steel can be predicted by substituting this parameter into the mathematical model suggested for this purpose. This generalized model makes it possible to establish the correlation of the structure, composition, state, and properties on the one hand and the metal behavior in machines on the other. Figures 1; tables 1; references 10.

Local Carburizing of Eutectoid Instrument Steel

937D0029E Moscow IZVESTIYA VYSSHIKH UCHEBNYKH ZAVEDENIY: CHERNAYA METALLURGIYA in Russian No 4, Apr 92 pp 53-54

[Article by V.I. Alimov, V.G. Onopriyenko, V.Ya. Yavorskaya, Donetsk Polytechnic Institute; UDC 669.15-194.2.056]

[Abstract] Traditional and nontraditional carburizing of structural low carbon steels and case-hardening of the dies and punches from hypo- and hypereutectoid steels are discussed, and the possibility of increasing the wear resistance of the working surfaces of ShTs-Sh-400—1,000 calipers from the U8A eutectoid carbon steel by carburizing is assessed. To this end, samples of strips of steel U8A whose size corresponds to the 15x20 mm initial caliper blank dimensions are examined. In the initial state, the steel has a mixture of flaky pearlite with a 60/40 spheroidization degree and an HB 197 hardness; the carburizing process is conducted in a SNOL-16.2,5.1/9 furnace at a 900+/-10° C for 2, 5, and 8 h. The zones containing more than 0.8 percent C and zones differing in the grain size are determined metallographically; the sample microstructure is examined under Neophot-21 and MMR-2 microscopes and the microhardness is measured by a MMT-3 tested under a 0.5 N load; the hardness is measured by a Rockwell hardness gauge while wear resistance tests are carried out in a DL-M1 machine using abrasive particles. A structural diagram of the carburized layer is cited, and the dependence of the layer depth and zone width as a function of the carburizing duration, the transverse grain size in the case-hardened layer and in the sample core as a function of the saturation duration, and the mass loss as a function of the abrasion condition and wear path length are plotted. The formation of a cementite grid on the grain boundaries and cementite flakes under an extended exposure is reported, and it is noted that case-hardening makes it possible to increase the wear resistance of calipers and extend their warranty life by 1.5 times while preserving the accuracy parameters. Carburizing can be used not only for instruments but also for hard thin-walled products which require an elevated localized wear resistance, i.e., small die tools. Figures 4; references 7.

Self-Regulation of Decarburization Reaction in Open Hearth Furnaces

937D0029H Moscow IZVESTIYA VYSSHIKH UCHEBNYKH ZAVEDENIY: CHERNAYA METALLURGIYA in Russian No 4, Apr 92 pp 89-91

[Article by L.V. Kamkina, Yu.N. Yakovlev, Dnepropetrovsk Metallurgical Institute; UDC 669.183.2]

[Abstract] The irreversibility of the decarburization process which occurs in an open system is noted, and an attempt is made to examine the nonequilibrium decarburization process on the basis of a mathematical model which takes into account the impurity transport and distribution in the melt volume. The model is based on partial differential equations of large-scale oxygen transport in the slag and metal with source terms. A second-kind boundary condition on the gas/slag interface is formulated, and the decarburization process is represented as three principal reactions. The effect of individual factors on the self-regulation of the decarburization process is examined using the example of a 500 t open hearth furnace; to this end, the correlation of the temperature behavior during the refining and the decarburization rate is investigated. The temperature behavior, carbon concentration in the metal, and carbon monoxide content in the slag, the dependence of the chemical affinity on the carbon concentration, the relative oxygen flow and entropy production, and the thermodynamic resistance variation are plotted. An analysis of the irreversible decarburization process all of whose links are far from equilibrium and fall within the nonlinear area shows that self-regulation amounts to a redistribution of the oxygen potential inside the system with a change in the resistance of one process link so as to ensure that the maximum potential difference at a given carbon concentration remains constant while the sum of oxygen flows to individual links is equal to the total flow entering the system. Figures 3; references 4.

Structure and Physical Property Characteristics of Liquid Pig Iron and Their Interrelation With Structure and Service Properties of Castings

937D0030A Moscow IZVESTIYA VYSSHIKH UCHEBNYKH ZAVEDENIY: CHERNAYA METALLURGIYA in Russian No 3, Mar 92 pp 1-5

[Article by Ye.Ye. Tretyakova, B.A. Baum, G.V. Tyagunov, T.K. Kostina, M.V. Rovbo, Urals Polytechnic Institute; UDC 621.74.043]

[Abstract] The proceedings of a national conference on the Interrelation of Liquid and Solid Metal States held on 1-7 Apr 91 in Sochi are discussed; in particular, the interrelation of the polytherms of the physical properties of liquid pig irons and their structural characteristics in the solid and liquid states is analyzed, and the behavior of surface tension, kinematic viscosity, and resistivity of grey cast iron in the liquid state is examined. To this end, an X-ray diffraction and differential thermal melt analyses are carried out, and the oxygen concentration in the samples before and after the tests is analyzed. The effect of the maximum smelting temperature of foundry pig iron on the character of melt surface tension polytherms under heating and cooling, kinematic viscosity and resistivity polytherms of foundry pig iron in the liquid state under heating and cooling, the effect of the maximum melt heating temperature on the dependence of the reflected X-radiation intensity on the foundry pig iron angle of reflection, the effect of the temperature on surface tension and carbon modification form in liquid cast iron during heating and cooling, and the effect of the maximum smelting temperature on the graphite inclusion form are plotted. An analysis of the polytherms makes it possible to delineate the ranges of significant structural variations and select the melt treatment parameters depending on the structural requirements. The polytherms are typical of high-carbon melts. By selecting the optimum temperature conditions, one can control the melt state prior to solidification as well as affect the solidification mechanism and form the necessary solid metal structure. Figures 7; tables 1; references 4.

Kinetic Characteristics of Magnetite Concentrate Reduction in Rotary Magnetic Field

937D0030B Moscow IZVESTIYA VYSSHIKH UCHEBNYKH ZAVEDENIY: CHERNAYA METALLURGIYA in Russian No 3, Mar 92 pp 6-8

[Article by D.I. Ryzhonkov, A.P. Kolgin, S.B. Kostyrev, A.V. Vasilyev, A.B. Savin, V.M. Pak, Moscow Steel and Alloy Institute; UDC 669.094.1:553.311]

[Abstract] The reduction kinetics of Olenegorsk Ore Dressing Works (GOK) magnetite concentrate containing 72 percent Fe and <1 percent impurities is examined in a fluidized eddy bed unit (AVS) where a rotary magnetic field is applied to the ferromagnetic material. The concentrate is reduced with hydrogen within a 626-803K range and the degree of reduction is determined gravimetrically. The experimental dependence of the Olenegorsk concentrate reduction degree on the reduction duration and temperature, the fraction composition of the Olenegorsk concentrate, and the dependence of the chemical reaction rate constant on temperature according to the particle distribution by the equivalent radius and a weighted average particle radius—the two approaches used in determining the kinetic parameters—are plotted. A computer software package with graphic applications is developed for determining the rate constant using Mekewan's equations. The study demonstrates that the concentrate reduction in the eddy layer within the temperature range under study is better described by a system containing Mekewan's equations allowing for the charge polydispersity compared to the calculations made for the weighted average size and Seth's and Ross's equations. Figures 3; tables 1; references 5: 3 Russian, 2 Western.

Investigation of Reaction Kinetics During Fe Reduction With Composite Gaseous Mixtures

937D0030C Moscow IZVESTIYA VYSSHIKH UCHEBNYKH ZAVEDENIY: CHERNAYA METALLURGIYA in Russian No 3, Mar 92 pp 11-13

[Article by V.K. Simonova, S.Ye. Lazutkin, L.N. Rudenko, V.M. Ostrovskiy, Ye.N. Vasilyev, N.N. Ostroukh, Dnepropetrovsk Metallurgical Institute and Central Scientific Research Institute of Ferrous Metallurgy; UDC 669.094.1'2:66.092]

[Abstract] The lack of data on the kinetic patterns of gaseous reduction of iron ore materials in the flow of natural gas oxidation conversion products and the concomitant reactions prompted a study of the reduction kinetics of pellets used at the Oskol Electrometallurgy Works (OEMK) and the attendant processes within a 700-900° C temperature range. The gas composition corresponds to the commercial converter gas with or without methane; the latter is added in various amounts in the form of natural gas from the Shebelinsk deposit with 94 percent CH_4. The volume rate of the gas delivered to the reactor is measured by flow meters while the kinetics are monitored by analyzing the gaseous pellet metallization products using a Gazokhrom-3101 chromatograph. The effect of temperature on the pellet reduction kinetics using converter natural gas and the iron recarburization during the process and the effect of temperature on the pellet reduction kinetics using converter gas with 5 percent and 10 percent CH_4 and iron recarburization during the process are plotted. The thermodynamic analyses are carried out on a YeS-1045 Unified Series computer using a routine developed by the authors. The method makes it possible simultaneously to monitor the development of oxide phases and associated iron carburization reactions and the methane formation and conversion. The kinetic iron reduction patterns are closely related to the development of concomitant reactions whose rate, in turn, depends both on the gaseous phase component concentration and temperature. Figures 3; references 3.

Structure Formation of Steel Blooms During Solidification Under Continuous Casting

937D0030D Moscow IZVESTIYA VYSSHIKH UCHEBNYKH ZAVEDENIY: CHERNAYA METALLURGIYA in Russian No 3, Mar 92 pp 21-25

[Article by V.V. Sobolev, P.M. Trefilov, I.N. Shifrin, A.R. Bakkal, N.G. Romanova, Novosibirsk Branch of the Scientific Production Association of the All-Union Institute of Light Alloys; UDC 669.18:621.746.5.047]

[Abstract] The theoretical analysis of the crystal structure formation of steel 45 blooms under continuous radial casting (RNL) with electromagnetic agitation (EMP) with the help of two 600 mm long magnetoelectric generators positioned along the ingot height which began in an earlier issue of this journal (No. 1, 1992) is continued. Attention is focused on the extent of the dendritic structure zones on the side of the smaller and greater ingot radii and the smaller face, respectively, and the dimensions of the central zone of equiaxial crystals in the greater and smaller ingot face directions of a 300x360 mm ingot during continuous radial casting. The ingot's dendritic structure is considered in detail, and formulae are derived for calculating the temperature and solidification rate gradients. The dependence of the ingot structure zones and differences between them on the generator spacing is summarized. The dependence of the structure inhomogeneity parameters on the second generator position and the distributions of the spacing between the secondary dendrite branches and first-order dendritic axis thickness with either or both generators in operation are plotted. The development of gas shrinkage porosity during continuous radial casting in general and axial porosity in particular are examined. The relative pore volume, radius, and density distribution in the St3 ingot is analyzed. The dependence of the axial porosity on the generator condition is tabulated, and it is shown that the use of both generators leads to an increase in the relative pore volume and density and a decrease in their radius on the ingot axis. Electromagnetic agitation refines the pores and increases their relative volume which, in the end, improves the cast metal structure since porosity becomes more scattered and can be easily eliminated by subsequent working. Figures 3; tables 3; references 9.

Solidification and Structure-Formation Process Characteristics of Slabs Cast in Curvilinear Continuous Casting Machines

937D0030E Moscow IZVESTIYA VYSSHIKH UCHEBNYKH ZAVEDENIY: CHERNAYA METALLURGIYA in Russian No 3, Mar 92 pp 25-28

[Article by N.I. Revtov, O.B. Isayev, O.V. Nosochenko, V.V. Yemelyanov, I.G. Nikolayeva, Mariupol Metallurgical Institute; UDC 621.746:669.18]

[Abstract] The excessive metal outlays in making slabs and plates by rolling from ingots cast into molds and the difficulty of using continuously cast slabs due to the problem of producing cast metal with a sufficiently uniform structure and good mechanical properties of the rolled items at low reduction values prompted an investigation into the characteristics of the solidification and structure formation processes of continuously cast 250x1,650 and 300x1,850 mm slabs produced in curvilinear continuous casting machines with an addition of steel band-shaped macrorefrigeators. The steel St3sp and 09G2S casting rate was manipulated within 0.6-0.8 m/min at a metal temperature in the pony ladle of 1,520-1,550° C. The melt temperature in the upper part of the mold was measured during the experiment by a special floating unit with inertial thermocouples. The averaged temperature gradient values in the solid skin cross section are calculated using temperature probing data. The dependence of the solidification ratio of the mold radius to the square root of the solidification rate on the distance below the metal meniscus and the behavior of the ratio in pilot and commercial slabs are plotted. The effect of the steel bands with various chemical composition on the slab macrostructure is discussed, and the effect of macrorefrigerators on the continuously cast slab structure is examined graphically. The patterns of slab solidification rate as a function of the cast metal overheating and the optimum steel band mass rate parameters are established. Under the conditions which affect the structure to the greatest extent, the columnar zone extent decreases by four- to sixfold while the skin zone thickness increases by 1.5-3 times, and a developed globular crystal zone is formed, the dendritic structure becomes more dense, and the slab structure asymmetry decreases on the large and small radius sides. The addition of macrorefrigerators made it possible to improve the product quality by increasing the low carbon and low alloy steel ductility by 20-40 percent and toughness by 1.5-2.0 times. Figures 4; tables 1; references 11: 9 Russian, 2 Western.

Steel Degassing Characteristics Under Inert Gas Blasting in Ladle

937D0030J Moscow IZVESTIYA VYSSHIKH UCHEBNYKH ZAVEDENIY: CHERNAYA METALLURGIYA in Russian No 3, Mar 92 pp 87-88

[Article by A.S. Kondratyev, A.S. Aleksandrov, Ye.A. Balichev, Leningrad State Engineering University; UDC 669.046.517:66.096]

[Abstract] The difficulty of explaining empirical data on the efficiency of gas dynamic modules with an unconventional shape and a decrease in the hydrogen concentration in the melt from the viewpoint of traditional concepts of interacting gas jets and metal melts prompted a study of liquid steel St3 being blasted with argon in a 350 t pouring ladle through an immersible tuyere with a nontraditionally shaped nozzle. The melt was blasted for 5-7 min at an Ar rate of 0.03-0.05 m^3/t; the hydrogen concentration in the melt dropped substantially from 7-9 $cm^3/100$ g at the start of the blast to 3-4 $cm^3/100$ g at the end. A total of 11-18 m^3 of hydrogen was removed at a 10-17 m^3 Ar consumption. A discrepancy with published data can be resolved by assuming that long-lived cavitation voids which serve as an additional refining phase form in the melt under the effect of the supersonic gas get. It is shown that Ar is capable of directly removing no more than 0.7 m^3 H_2 while the remaining 9.8 m^3 H_2 is removed by the additional refining phase thus attesting to the high efficiency of using nontraditional gas dynamic modules in ladle refining. References 6: 5 Russian, 1 Western.

Membrane Refining as Method of Steel Deoxidation

937D0031A Moscow IZVESTIYA VYSSHIKH UCHEBNYKH ZAVEDENIY: CHERNAYA METALLURGIYA in Russian No 2, Feb 92 pp 1-5

[Article by V.Ye. Roshchin, A.A. Epov, V.P. Gribanov, Chelyabinsk State Engineering University; UDC 669.046:669.054.7]

[Abstract] The study of the possibility of removing oxygen from a metal melt through a solid electrolyte membrane with an anion conduction which began in this journal (No. 10, 1990) is continued, and an attempt is made to identify the limiting stages of the refining process and the likely ways of enhancing it. To this end, the membrane refining process is monitored by two methods: by a change on the oxygen activity in the deoxidized melt and by the resulting current in the external circuit. The effect of agitation on the deoxidation rate is examined using a special unit. The effect of the crucible rotation on the deoxidation kinetics, the behavior of the deoxidation rate under spinning, and the melt deoxidation at a high oxygen content are plotted for both methods (activity and current). The effect of the deoxidizer type on the deoxidation rate is investigated; in particular, the effect of the state of aggregation of the deoxidizing agent on the deoxidation rate, the effect of the deoxidation products on the deoxidation rate for a liquid agent, and the comparative kinetics of deoxidation by graphite and ferrozirconium and aluminum are plotted. An analysis shows that starting with the eighth or tenth minute of deoxidation under stirring, the oxygen removal rate is limited by the mass transfer in the melt; it is speculated that at the start of deoxidation, the oxygen removal rate is controlled by the formation of an immiscible layer near the refined melt's interface with the solid electrolyte membrane. Gaseous deoxidation products have the least negative effect on the process while solid deoxidation products poison the membrane and worsen the refining conditions. Figures 7; references 4: 2 Russian, 2 Western.

Assessing Possibility of Direct Uses of Blast Furnace Conversion Pig Iron for Making Wear Resistant Milling Bodies

937D0031B Moscow IZVESTIYA VYSSHIKH UCHEBNYKH ZAVEDENIY: CHERNAYA METALLURGIYA in Russian No 2, Feb 92 pp 7-9

[Article by V.I. Shatokha, V.M. Snagovskiy, Yu.P. Martynov, O.V. Sotsenko, I.B. Kruglov, Dnepropetrovsk Metallurgical Institute; UDC 669.162.275.1:621.746.58]

[Abstract] The possibility of making parabolic milling bodies of two sizes from blast furnace conversion pig iron by casting into knock-down metal molds in a casting machine for use in ore grinding devices is examined. The pig iron composition and HRC hardness at a 3 mm depth from the cast surface of milling bodies made at two locations are summarized. The hardness behavior in the mean cross section of paraboloid milling bodies cast directly from the blast furnace and after remelting in an induction furnace and treatment with various compositions is plotted. The ladle refining conditions, the initial and final composition of pig iron, and the properties of milling bodies from five experimental batches are examined, and the microstructure of the samples is cited. Methods of suppressing graphitization are reviewed, and the effect of various additions on the microstructure and properties is investigated. An analysis shows that paraboloid grinding bodies cast directly from the blast furnace runner are better than those from the cupola; the necessary hardness level can be attained by preliminary ladle treatment with chilling additions but may also be reached by adding oxidizing reagents, such as mill scale. Figures 2; tables 2; references 1.

Development of Efficient Range of Resource-Saving Products for Ladle Deoxidation of Steel

937D0031C Moscow IZVESTIYA VYSSHIKH UCHEBNYKH ZAVEDENIY: CHERNAYA METALLURGIYA in Russian No 2, Feb 92 pp 12-14

[Article by V.A. Vikhlevshchuk, Yu.F. Vyatkin, I.A. Pavlyuchenkov, V.A. Kondrashkin, S.Ye. Samokhvalov, G.N. Chernomaz, Dnepropetrovsk Ferrous Metallurgy Institute; UDC 669.046.554:669.71]

[Abstract] The inefficiency of using large aluminum pigs as a deoxidizing agent due to its prolonged reaction with the slag and heavy losses prompted an attempt to switch to smaller aluminum products for ladle deoxidation of steel and adapt the process to automated control. To this end, the life span of the aluminum spherical granules with various diameters in the casting ladle with killed low carbon and high carbon steel is simulated by mathematical modeling in order to find an efficient granulometric composition of resource-saving aluminum products. The mathematical model and the underlying assumptions are described and a schematic diagram of the solid melting area in the liquid melt is cited. The amount of heat released during the melting of Al in killed steel is calculated, and the behavior of the aluminum melting duration in low and high carbon steel is plotted. The study makes it possible to determine the optimum time for adding the deoxidizer to the ladle during the tapping; it is shown that addition of granules to the metal jet is 1.5-2.8 times more efficient that addition of pigs. A 5 to 20-30 mm granulometric composition of aluminum is suggested. The computation program is written in the Pascal language for an XT/AT microcomputer. Figures 2; references 3.

Steelmaking Pool Boil

937D0031D Moscow IZVESTIYA VYSSHIKH UCHEBNYKH ZAVEDENIY: CHERNAYA METALLURGIYA in Russian No 2, Feb 92 pp 16-20

[Article by V.B. Okhotskiy, Dnepropetrovsk Metallurgical Institute; UDC 669.18]

[Abstract] The availability of new research data on the carbon oxidation process and the resulting steelmaking pool boil and better understanding of diffusion kinetics prompted a reexamination of the steelmaking pool boil and attendant phenomena. The bubble formation on the metal/lining interface during the carbon oxidation process and the carbon monoxide bubble formation on the metal contact boundary with the wall material are investigated, and the mass transport processes in the liquid metal pool are analyzed. Material balance equations and formulae for calculating the mass transfer coefficients are derived on the basis of hydrodynamic and mass transfer principles. These equations make it possible to evaluate the boil process and determine the bubble formation parameters and their flotation as well as calculate the concentration gradients in the reacting phases. The conclusion is drawn that the process of complex oxygen transfer in the rimmer is limited by gaseous phase transport during most of the refining stage; this explains the more or less constant carbon burnout rate during this phase. Oxygen inflow to the slag from the charge or the interaction zone during the blasting temporarily boosts the oxygen transport; during converter processes, this is virtually the only pool boil source beyond the interaction zone. References 20: 13 Russian, 7 Western.

On Metallurgical Value of Ferrous Metal Scrap

937D0036B Moscow LITEYNOYE PROIZVODSTVO in Russian No 7, Jul 92 pp 9-11

[Article by A.T. Shipulin, Lipetsk Polytechnic Institute; UDC 621.745.012]

[Abstract] The need to analyze the effect of the metal scrap and ferrous metal waste on the behavior of the technical and economic indicators of the ready metal necessitated a search for data on the individual types of scrap and waste used in various steelmaking vessels. The metallurgical value coefficient which is determined by the ratio of outlays for making a unit of metallurgical production of the same quality from primary raw materials (blast furnace pig iron) to that of the replacement secondary ferrous metal is selected as such an indicator. The metallurgical value coefficient of various types of scrap and secondary ferrous metal waste in relation to liquid conversion pig iron determined at the All-Union Central Scientific Research Institute of Secondary Ferrous Metals are summarized, and a formula is derived for calculating the selling price for standard types of steel scrap and waste according to 1 Aug rates. Comparative data on individual types of lump scrap are tabulated. Scrap and waste utilization experience shows that the smaller the scrap piece size, the higher the probability of nonmetallic extraneous impurities getting into the scrap. Consequently, it is suggested that GOST 2787-75 be revised. The effect of the proportion of malleable and grey pig iron in the charge and the resulting difference in the graphite inclusion size on the casting strength is discussed, and it is suggested that pig iron scrap and waste be divided into two categories (with a $\leq$20 and $\leq$40 kg weight). The need for soliciting the opinion of foundry workers and designers in developing a new standard is stressed. Tables 2; references 3.

Casting Austenitic Steel for Cryogenic Engineering

937D0036C Moscow LITEYNOYE PROIZVODSTVO in Russian No 7, Jul 92 pp 13-14

[Article by S.L. Gorobchenko, B.B. Gulyayev, Refrigeration Engineering Institute and GTU; UDC 621.74:669.14]

[Abstract] The methods of increasing the low cold resistance of casting steels which prevents their use in cryogenic engineering and reducing the impurity segregation along the grain boundaries are considered; attention is focused on improving the impurity solubility in the metal matrix. The limit of C, O, N, H, P and S impurity solubility in Fe, Cr, Ni, and Mn at a low temperature is summarized, and the Fe-Cr-Mn constitution diagram after water quenching at a 1,100° C temperature is plotted. A mathematical model of the impurity solubility in the matrix is derived, and the chemical composition of 10 pilot smeltings and their mechanical properties without and with heat treatment as well as fluidity are examined. The maximum toughness within a cryogenic temperature range is selected as the optimization criterion and the results of comparative tests of valves made by investment casting from steels 12Kh18N10T, 12Kh18N10TL, and 07Kh8G28L, i.e., breaking pressure and diameter increase, are presented. Based on tests data, steel 08KhG28L is chosen for making cryogenic valves with vacuum insulation at the Kriogenmash Scientific Production Association resulting in savings of 650 rubles per ton. Figures 1; tables 4; references 2.

Structure and Properties of TiC-Steel G13 Alloys

937D0029D Moscow IZVESTIYA VYSSHIKH UCHEBNYKH ZAVEDENIY: CHERNAYA METALLURGIYA in Russian No 4, Apr 92 pp 51-53

[Article by S.N. Kulkov, O.V. Yablokova, Strength Physics and Materials Science Institute at the Siberian Department of the USSR Academy of Sciences, Tomsk; UDC (669.15'74-194+669.295'784):546.3-19]

[Abstract] The effect of the composition and properties of the binding phase on the performance of sintered carbide steels is discussed, and it is noted that the presence of a large amount of carbide phase in TiC-steel alloys affects the phase transitions and structure of the steel binder as well as its properties. This prompted a study of the structure and property behavior of TiC-steel G13 alloys as a function of the TiC concentration. To this end, alloys containing 30-70 percent TiC (by volume) are examined. A TiC powder produced by reduction and a steel powder made by spraying are alloyed by powder metallurgy, and compacted samples are sintered in a helium atmosphere at a 1,625-1,725K temperature, depending on the TiC concentration in the alloy, and by isothermal exposure for one hour. A metallographic study shows that the microstructure during sintering in the presence of the liquid phase depends significantly on the alloy composition. A bar chart of the carbide grain size distribution, the lattice constant variations of TiC and γ- and α-Fe and the phases' X-ray intensity ratio as a function of the TiC concentration in the alloy, the dependence of the alloy hardness and bending strength on the TiC volume fraction, and the behavior of the alloy wear resistance as a function of the TiC component content are plotted. An analysis demonstrates that the carbide component greatly affects the steel binder structure, phase transitions in it, and thus, the alloy properties as a whole. Figures 4; references 6.

Low-Waste Production Practices at Dzhezkazgan Copper Smeltery

937D0033A Moscow TSVETNYYE METALLY in Russian No 9, Sep 92 pp 14-16

[Article by A.N. Kvyatkovskiy, T.M. Urumov, T.M. Abdrakhmanov, V.M. Bobrov, N.I. Ilyasov, V.G. Polyanskiy, Scientific Production Association of Dzhezkazgan Nonferrous Metals and Metallurgy and Dressing Institute at the Kazakh Academy of Sciences; UDC 669.33]

[Abstract] The possibility of developing a low-waste method of processing high-silica and low-iron copper concentrates prompted the development of a low-waste technology of removing the Altay pyrite and Cu-Fe concentrates from the electric melting charge and quartz ore—from the converter process. The specific features of the method are described, and it is noted that about 20-25 percent of the dump slag can be used in the liquid form as the quartz flux in converting high-grade matte, with additional smelting in the converter; the remaining 75 to 80 percent can be used for making mineral wool and filling mine workings. The technology has been under development since 1987 at the Scientific Production Association of Dzhezkazgan Nonferrous Metals and Metallurgy and Dressing Institute at the Kazakh Academy of Sciences; it made it possible to increase the copper concentration in the matte from 47.3 to 57.6 percent and to reduce the dump slag production by 26 percent and reduce the converter slag by 42 percent per ton of copper. The electric power consumption per ton of charge remains virtually unchanged. The effect of the removal of Cu-Fe concentrated from the charge on the technical and economic indicators of the copper smeltery are summarized, and the conclusion is drawn that the theoretical foundation of waste-free Dzhezkazgan copper concentrate processing is confirmed by the early stages of the low-waste method implementation. The technology is suitable for smelting a copper charge containing slag with 22-25 percent CaO to produce high-grade matte; to date, the method has enables the Dzhezkazgan smeltery to increase the copper recovery into crude metal of up to 98.3 percent, increase the electric furnace efficiency, lower electric power outlays by 320 kWh per ton of blister copper, and improve the working conditions. Tables 1; references 4.

Development of Slag Impoverishment Technology Using Copper Clinker

937D0033B Moscow TSVETNYYE METALLY in Russian No 9, Sep 92 pp 19-21

[Article by F.A. Myzenkov, V.V. Mechev, A.I. Tertichnyy, O.V. Glupov, O.V. Vlasov, State Nonferrous Metals Institute; UDC 669.33:669.054.82]

[Abstract] The need to impoverish rich autogenous and converter slags in nonferrous metal smelting and the shortcomings of traditional impoverishment methods, particularly with respect to ensuring production of high-grade gases suitable for sulfuric acid production, prompted the development of converter and autogenous process slag impoverishment using top oxygen-bearing blast and copper clinker from zinc smelteries. The study is carried out at the Pilot Experimental Plant of the State Nonferrous Metals Institute in Ryazan (POEMZ) and is aimed to deep slag impoverishment and production of process gases which do not call for subsequent removal of sulfur dioxide. The process is based on the principle of producing a metallized melt which retains sulfur in the matte while selectively oxidizing carbon on the pool surface. The Ust-Kamenogosrsk zinc smeltery (UKSTsK) clinker and copper smeltery slags from the Altay Mining and Metallurgy Works (AGMK) are used for tests in a 5 ton ROEMZ vertical converter. The testing procedure which resulted in lowering the copper content in the converter slag in addition to sharply decreasing the concentration of Ag and Au to 5 and 0.2 g/t, respectively, is outlined in detail. Cu, Au, and Ag recovery to the matte amounted to 92.5, 97.0, and 95.7 percent, respectively. The process is recommended for

impoverishing hot converter slag in individual fixed units with top blast in a continuous operation. It is noted that a similar technique can be used to impoverish the KFP slag. The use of clinker for slag impoverishment makes it possible efficiently to use the reduction potential of the solid reducing agent and the metallized part of iron. When only the solid reducing agent is used, it should also serve as the metallized part of iron. Tables 3; reference 8.

Effect of Temperature on Interaction Kinetics of Sulfur and Oxygen Dissolved in Copper

937D0033C Moscow TSVETNYYE METALLY in Russian No 9, Sep 92 pp 21-23

[Article by M.T. Zhunusov, S.V. Sukharev, A.L. Kozhanov, A.I. Oruzheynikov, NGMK; UDC 669.33]

[Abstract] The effect of the oxidation character of copper sulfide dissolved in the metallic phase in the presence of impurities, i.e., at the concluding copper smelting stage, on the quality of blister copper produced by converting a Ni-bearing sulfide copper feedstock is discussed, and an attempt is made to determine the effect of temperature on the interaction kinetics of S and O_2 dissolved in copper and the behavior of sulfur. To this end, the temperature dependence of the concluding phase reactions is examined in a Setaram differential thermal analysis unit. A charge sample batch is heated in an alundum crucible which is evacuated and filled with He, then heated either at a constant rate or to a fixed temperature with subsequent isothermal exposure until the mass equalizes. The behavior of the sample batch weight at a constant heating rate in a helium atmosphere, the sample mass variation with temperature, the temperature variation per 1 mg of sample mass change at the concluding oxidation stage, and the melt mass behavior at various temperatures are plotted. The findings indicate that melt is quite sensitive to temperature variations during the sulfur oxidation from the copper melt in the presence of copper sulfide within a 10 percent copper sulfide concentration range. In the dynamic mode, this interaction is determined by the sulfur concentration in the melt while static conditions make it possible to identify the relationship between the sulfur removal rate and the presence of impurities. Figures 4; references 8.

Sulfur Distribution Between Ca-Bearing Oxide Melt and Nickel

937D0033D Moscow TSVETNYYE METALLY in Russian No 9, Sep 92 pp 23-25

[Article by L.N. Shekhter, V.G. Leontyev, M.A. Sulimov, S.O. Boykov, Metallurgy Institute at Russian Federation Academy of Sciences; UDC 669.243]

[Abstract] The failure to utilize the high sulfur-absorbing capacity of nonferrous oxide melts and slags in nickel and copper pyrometallurgy prompted a study of the sulfur distribution between nonferrous metals and the slag. To this end, the interphase sulfur distribution between Ni and the C-bearing oxide melt is examined using NO-grade electrolytic Ni, OCh-grade elementary sulfur, and Ch-grade calcium and silicon oxides. The slag is additionally smelted from the components in an induction furnace in a graphite crucible at a 1,500° C temperature. The study is carried out using radioactive tracers (RAI) and S irradiated with β-rays in a CW mode is mixed with Ni and heated in a vacuum. The β-radiation intensity variation of Ni samples as a function of temperature and the temperature dependence of the equilibrium distribution coefficient are plotted. The rate parameters of the sulfur redistribution between the nickel and slag melts is summarized. The distribution coefficient depends on temperature significantly and increases by almost tenfold with an 85° temperature change. The enthalpy and entropy of S transition from the metal to the slag are 640 kJ/mole and 360 J/mole x deg. It is noted that the thermodynamic characteristics found in the study should be treated as estimates and the need for additional experiments is stressed. It is stated nevertheless that the high-temperature low-nickel melt desulfurization technology is a promising one. Figures 2; tables 1; references 3: 2 Russian, 1 Western.

Chlorination Patterns of Elementary Gold and Its Natural Primary Sources

937D0033E Moscow TSVETNYYE METALLY in Russian No 9, Sep 92 pp 26-27

[Article by M.N. Zyrnov, Irkutsk Polytechnic Institute; UDC 669.636]

[Abstract] The behavior pattern of elementary Au chlorination by gaseous Cl as a function of temperature is studied, and the flaky gold chlorination rate as a function of temperature and duration and the change in the degree of metal chlorination from natural primary sources as a function of temperature are plotted. The gold chlorination reaction commences at 140-180° C and the transfer degree increases until a 250-275° C temperature after which the chlorination degree drops and ceases at 500-650° C. The interaction restarts again above 650° C and the chlorination degree increases with temperature. The Gibbs energy and reaction constant of Au chlorination with ferrous and ferric chlorides are summarized. The findings show that the gold chlorination degree increases steadily in the case of auriferous concentrates in contrast to elementary Au due to the release of active atomic Cl which, in contrast to molecular chlorine, interacts with Au within a broad temperature range which includes the 500-650° C interval in which Au does not react with chlorine molecules. In the case of natural raw material chlorination, SO_2, CO, H_2O, and As_2O_3 pass to the gaseous phase. Figures 2; tables 2; references 6.

On Rhenium Condensation on Dust From Vanyukov Smelting Gases

937D0033F Moscow TSVETNYYE METALLY in Russian No 9, Sep 92 pp 45-47

[Article by A.D. Besser, I.V. Miroyevskaya, State Nonferrous Metals Institute; UDC 669.29.819.7]

[Abstract] A method of Re recovery from converter gases in the wet scrubbing system of H_2SO_4 production with subsequent Re extraction from the solution by sorption was used for the first time in the world at the Balkhashmed Production Association (the former Balkhash Mining and Metallurgy Works) in the course of copper raw material processing yet most of Re was lost irreversibly with flue gases and slags during the reverberatory smelting. This prompted an investigation into the process of Re condensation on dust from Vanyukov smelting gases. To this end, the effect of gaseous phase temperature on Re condensation on dust particles without air suction is studied in an enlarged lab experiment whereby a dust-and-gas mixture is sampled directly from the gas duct of the PV-1 commercial Vanyukov furnace at the outlet from the waste heat recovery boiler. The experiment procedure is outlined and the dependence of Re condensation from Vanyukov smelting gases on dust on the process temperature is plotted. The balance error did not exceed 9-15 percent. The study shows that Re losses are $\leq$10-15 percent within a 350-400° C range and its principal fraction may be concentrated in the flushing acid and recovered into commercial ammonium perrhenate. Yet as the gas temperature decreases, Re losses with dust rise exponentially and exceed 50 percent at 250° C. This confirms the technological necessity of ensuring a temperature of at least 350° C in the gas path and minimizing air intake due to suction. Figures 1; references 3.

Continuous Casting of Copper Alloys Into Graphite Molds

937D0036G Moscow LITEYNOYE PROIZVODSTVO in Russian No 7, Jul 92 pp 22-23

[Article by V.V. Dembovskiy, A.A. Yatsenko, Yu.V. Pushkarev, Northwestern Correspondence Polytechnic Institute and Proletarskiyy zavod Production Association; UDC 621.746.27]

[Abstract] The experience of continuous casting of copper alloys at the Proletarskiyy zavod Production Association in St. Petersburg in two units, a horizontal machine developed at the Ukrainian Scientific Research Institute of Metallurgy and a vertical unit for making round blanks, primarily from bronze, is summarized; the issue of selecting the rate at which the billet is extracted from the mold is addressed. The problem of developing an adequate mathematical model of the process and determining the casting parameters, including the casting rate, is formulated. An explicit difference procedure ensuring a Schmidt-wise solution stability is used as the computational technique. The study reveals that the analytical values of the temperature in the Br010F1 ingot differ little from experimental data. Formulae are derived for determining the stressed state of the billet and finding a set of finite difference values for cylindrical blanks. The problem is solved on a Unified Series (YeS) computer, and the mechanical properties of the part are determined at each time moment in each point on the net and compared to the permissible values. The time interval which determines the necessary minimum duration of the ingot stay in the mold, i.e., the casting rate, is determined on the basis of these relations. References 5.

Parameters of the Structure of Macroporous Glasses

927D0237A Moscow STEKLO I KERAMIKA in Russian No 7, Jul 92 pp 6-7

[Article by Yu. N. Kryuchkov, Institute of Technical Thermophysics, Ukrainian Academy of Sciences; UDC 666.3.022.69:539.27:541.183.02]

[Abstract] To make adsorbents with prescribed properties, sodium-borosilicate glass is treated with acid and then alkali to dissolve the unstable borate phase and make the glass porous. It is important to study parameters of the porous structure of these materials to optimize their manufacture and to predict their performance life and characteristics. A model of randomly arranged circles and the theory of percolation were used to derive formulas to determine parameters of the porous structure of these materials in a two-dimensional system. The theory of percolation was used to determine the critical volumetric content of the leached borate phase in borosilicate glass. It was found that the volume of the chemically unstable borate phase in the glass to be treated should be at least 29 percent. Another key parameter is the distribution by size of radii of necks that are formed where circles (spheres) intersect. A system of equations is proposed which helps to determine the distribution of volumes of pores according to the sizes of their necks, and a method is developed for correcting the porometric distribution curve for pore volumes according to the sizes of the necks that limit them.

Conductance of Glass Ceramic

927D0237B Moscow STEKLO I KERAMIKA in Russian No 7, Jul 92 p 8

[Article by M. A. Magrupov, A. V. Umarov, Sh. R. Khamidov, and R. Kh. Makhmudov, Tashkent State University; UDC 537.311.32:666.263.2]

[Abstract] Results of investigation of the conductance of the glass ceramic STsNK and of the character of current transfer in it are presented. Tests showed that sintering the material increases its conductance, which is due to the appearance of new conduction electrons as a result of formation of crystalline phases, and that the conductance of sintered STsNK depends significantly on temperature. To analyze the temperature dependence of conductance, the method of reduced activation energy was used. It was found that in the temperature range 200-500 K, there are three characteristic regions of temperature dependence of conductance. In the middle, transitional region, there is a break in the temperature curve which corresponds to a drop in the activation energy of conductance as the temperature drops. The drop in activation energy at low temperatures is apparently connected with a subsequent change in the conductance mechanism. Investigation of the frequency dependence of conductance showed that conductance increases as the frequency of change in an electrical field applied to the material increases. Thus, sintered STsNK possesses an ordered structure; with an increase in voltage from 20 to 400 volts, the voltage coefficient of specimens made of it is equal to a 30 percent change in their electrical resistance.

Synthesis of Glass Ceramics in the System Wollastonite-Apatite-Celsian

927D0237C Moscow STEKLO I KERAMIKA in Russian No 7, Jul 92 pp 9-11

[Article by T. A. Abduvaliyev, T. U. Uskakov, B. O. Yesimov, and B. O. Baydibekova, Kazakh Chemical Engineering Institute; UDC 666.263.2.002.3]

[Abstract] Compositions were tested for making glass ceramics on the basis of the pseudoternary system wollastonite-apatite-celsian, which are relatively abundant in nature and in industrial wastes. With a high melting point, celsian in glass ceramic compositions gives them high-temperature strength. The first step was to obtain transparent glasses which when heat-treated tend to undergo balanced crystallization. Vitrification in the system was investigated using model compositions. It was found that the transparent-glass region in the constitution diagram of the system takes in the wollastonite field and is limited by a molar content of 50 percent apatite and 50 percent celsian. Solid phase processes occurring during heat treatment of the mixture and processes of mineral formation that precede melting of the mixture in the temperature range 20-1200° C were investigated. It was found that processes of solid-phase mineral formation in glasses of all compositions differ substantially depending on the content of vitrifying oxides (SiO_2, P_2O_5), modifiers (CaO, BaO), and intermediate oxide (Al_2O_3).

Results of testing of five different compositions of the wollastonite-apatite-celsian system with varying contents of vitrifying oxides, modifiers, and intemediate oxide are discussed. The optimum composition consisting of 20 percent wollastonite, 30 percent apatite, and 50 percent celsian has a balanced crystallization with celsian as the main crystalline phase. It is made using slags from phosphorus production and barium concentrate to synthesize slag glass which when heat-treated in two stages produces glass ceramics which do not require costly raw materials.

Problems of Making Ceramics Thermally Stable, High-Strength and Heat-Resistant

927D0237D Moscow STEKLO I KERAMIKA in Russian No 7, Jul 92 pp 12-14

[Article by N. M. Bobkova, Belorussian Technological Institute; UDC 666.3/.7]

[Abstract] Trends around the world in developing specialty ceramic materials to meet rigorous performance requirements in high-temperature, high-wear conditions are reviewed. Development of new ceramic materials with high performance properties involves problems

associated with the purity of raw materials and their particle dimensions and the stability of processes for synthesizing them. New specialty ceramics can be made only with ultrapure and ultrafine powders which are synthesized using the sol-gel process and heat treatment, colloid dispersion by ultrasound and centrifuging, and gas phase reactions (plasma, laser) at high temperatures.

The author's institute has done research on developing ceramic materials based on oxynitride (Si_3N_4 + refractory oxides) and oxycarbide (SiC + refractory oxides) systems which make it possible to vary thermal conductivity, thermal stability and high-temperature strength of ceramics within broad limits while maintaining high mechanical strength. It was found that in oxynitride systems, mechanical strength on a level of 1000-1200 MPa is achieved only when powders with a specific surface of more than 15 m^2/gram are used. Materials with such strength have been obtained in oxynitride systems, and they possess a low thermal conductivity and a low thermal coefficient of expansion. However, mechanical strength and especially thermal conductivity are greatly affected by impurities whose presence is due to the method of obtaining starting materials. Impurities have a particularly pronounced effect on oxycarbide thermally conductive materials. For example, substantial differences have been found in the chemical composition of SiC made by the method of plasmochemical synthesis and by the method of self-propagating high-temperature synthesis. To develop ceramics with the required properties, it is necessary to be able to produce high-purity materials with a highly developed specific surface.

Ceramic Materials for Obtaining High-Purity Niobium and Tantalum Compounds

927D0237E Moscow STEKLO I KERAMIKA in Russian No 7, Jul 92 pp 14-15

[Article by A. A. Frolov, Institute of Materials Science Problems, Ukrainian Academy of Sciences; UDC 666.762]

[Abstract] In producing high-purity niobium and tantalum pentoxides, conventional corundum or quartz crucibles for firing the mixture have the drawback of contamination of the product with fluorine or chlorine compounds released due to chemical or mechanical erosion of the crucible material. A technique was developed for protective coating of large pieces of quartz ceramics with Nb_2O_5 in an optical furnace. The pieces are joined into container-type items and additional coating is applied to the seams.

A 4-liter vessel was made by this method and tested in industrial conditions. After 300 cycles (heating and cooling) of firing pre-dried niobium hydroxide, no cracking or flaking of the vessel's coating was detected. Next the vessel was tested over 1,200 cycles of firing niobium hydroxide with a moisture content of 30-50 percent and a fluorine content of 2 +/- 0.5 percent. Before these tests the thickness of the protective coating on the inside walls of the vessel was 2 mm, and after the tests with moist material its thickness had worn down to 0.5-1 mm due to peeling. Despite this, no contamination of the processed product with impurities from the vessel's walls was detected.

Hardening Porous Silicon Nitride Ceramics

927D0237F Moscow STEKLO I KERAMIKA in Russian No 7, Jul 92 pp 18-19

[Article by Ya. I. Belyy, V. V. Koleda, V. G. Malinin, V. A. Metlikin, V. M. Svistun, and S. A. Shlyakhov, Dnepropetrovsk Chemical Engineering Institute; UDC 666.762.93.002.237]

[Abstract] An effective way of hardening porous products made of silicon nitride ceramics is to introduce sintering additions by impregnating pores of already sintered products with inorganic salt solutions. Various methods were investigated for impregnating these ceramics with inorganic salt solutions which after thermal decomposition yield optimum compositions of the most frequently used sintering additions: oxides of magnesium, aluminum, and yttrium. The idea was to achieve a liquid-phase mechanism of sealing the impregnated material through formation, during a second firing of the product, of soda-lime and oxynitride glasses in which the indicated oxides and silicon dioxide play a part. After a detailed study of the thermal coefficient of expansion, the temperature at which softening begins, and the crystallization capacity of the glasses, impregnating solutions corresponding to them were prepared using nitrates of yttrium, magnesium, and aluminum. Specimens impregnated with them were fired at 873 K to achieve decomposition of the impregnating solutions to a mixture of oxides in pores, and they were then annealed in a nitrogen atmosphere at an optimum temperature for forming the liquid phase. Bending tests of the re-sintered specimens at room temperature showed that they all had become stronger as a result of the mechanothermal treatment, with some increasing in strength from 110 to 200 MPa.

Reasons for Glass Vial Packaged Drugs Being Contaminated With Glass Dust

927D0237G Moscow STEKLO I KERAMIKA in Russian No 7, Jul 92 pp 27-28

[Article by Yu. L. Belousov; UDC 666.176: 666.1.038.002.68]

[Abstract] The relationship between the quality of glass and conditions of manufacture of glass vials and the amount of rejects among glass-packaged drugs was investigated. Rejects considered were those that were judged so because of mechanical particles in the packaged solutions. Glass tubes from two medical glass factories were examined. It was found that in addition to dust formed by cutting the caps off glass tubes and being sucked down into the tube, dust can also form as a result of chemical inhomogeneity of the material of the glass tube. The appearance of glass dust in sealed vials due to inhomogeneous glass is explained as follows. When vials are formed, glass tubes are subject to thermal shock, which leads to formation of thermoelastic stresses of the first type. If the glass is not homogeneous, the thermoelastic stresses of the first type are augmented by stresses of the second type, which arise between adjacent sectors of glass with different chemical compositions and, consequently, different properties. When there is inhomogeneity, at temperatures over 10° C the total stresses result in the surface layers of vials breaking down and glass particles flaking off.

Optimization of Silicon Crystal Treatment by Floating Zone Melting

937D0033G Moscow TSVETNYYE METALLY in Russian No 9, Sep 92 pp 47-50

[Article by K.N. Neymark, Yu.V. Trubitsyn, I.F. Chervonyy, Zaporozhye Titanium Magnesium Smeltery; UDC 621.315.592]

[Abstract] The use of floating zone melting recrystallization (BZP) for making high-purity single crystals of semiconductor Si and the effect of B and P on the conduction type and resistivity (UES) are discussed, and a calculation procedure developed by the authors for various purposes is described. The proposed method is suitable for controlling the initial dopant concentration in silicon rods produced by hydrogen reduction of chlorides or thermal decomposition of monosilane, for determining the rod refining conditions by the floating zone melting recrystallization method in order to attain a specified resistivity and conduction type, and for producing single crystals with a uniform resistivity distribution in the cross section. The formulae are based on experimental-analytical techniques which approximate the real practical conditions to the utmost and are called upon to lower the outlays and increase ready product yield. Figures 1; tables 2; references 3.

The Production of a Cold-Rolled Strip From Precision Iron-Nickel Alloys

937D0003E Moscow STAL in Russian
No 7, Jul 92 pp 48-51

[Article by L.A. Agishev, V.Kh. Levinzon, G.Ye. Trusov, B.A. Filatov, and V.A. Bykov, Chelyabinsk Metallurgy Combine, Central Scientific Research Institute of Ferrous Metallurgy, and Metallurgy Scientific Research Institute; UDC 621.771.23]

[Abstract] The precision nickel-iron alloy 36N-VI is used in the production of picture tube masks. It has a very low temperature coefficient of linear expansion ($\alpha \leq 1.5 \times 10^{6}$ deg^{-1} at temperatures of 20 to 80° C). 36N-VI consists of 36 percent nickel, iron, and the required alloy-forming elements. The cold-rolled strips used to produce picture tube masks must be as wide as the screen and must be of even thickness to within 0.01 mm. The strips must also meet stringent requirements with respect to nonmetallic inclusions, roughness, and planarity and must be free of scabs, scratches, or other surface flaws. In 1979-1980 the Chelyabinsk Metallurgy Combine assimilated a modern process for producing cold-rolled strip from the invar precision alloys 42N and 47ND. Researchers have attempted to use the process to produce cold-rolled strips from 36N-VI. Preliminary laboratory tests confirmed the feasibility of producing 12.5-ton ingots on a blooming mill and 5.3-ton slabs on a 2300/1700 mill. The alloy was smelted in an ISV-25 vacuum induction furnace with a 12.5-ton-capacity crucible. The charges were calculated for the following percentages of basic elements: 0.009 percent C, 0.40 percent Mn, 0.20 percent Si, 36.0 percent Ni, and 0.10 percent Al. N1U nickel, 008Zhr and ZhChK low-carbon iron, A-97 aluminum, and a ferrocerium nickel-molybdenum-magnesium casting alloy were used as charge materials. The temperature measured 1,530° C after complete melting and 1,540° C before tapping. The sheets were rolled on 1250-2 and 1250-3 blooming mills and on a 2300/1700 mill. The alloy exhibited maximum plasticity at 1,200° C, so 1,170° C was selected as a rational process temperature. The rolling forces used were 40-45 percent less than those used with 12Cr18Ni10Ti steel 1,080 mm wide. Tests of the new procedure confirmed that the deformability of the alloy 36N-VI cast into ingots weighing 6.2 to 13.5 tons is entirely satisfactory when heated to temperatures up to 1,170° C and then rolled in accordance with the established regimen for corrosion-resistant steel. Processing the semiproduct stock in neutral-etching baths turned out to be problematic. Acid etching proved to be optimal. The required surface quality was achieved in the cold-rolled sheets by grinding to a depth of 0.1 mm with a thickness of 2-3 mm. Figures 4, table 1.

Manufacture of M6 and M8 Extra-Strong Bolts From Heat-Strengthened Carbon Rods

937D0003F Moscow STAL in Russian
No 7, Jul 92 pp 63-64

[Article by A.G. Rogovskiy, T.A. Verzhbitskaya, V.K. Likov, and Yu.V. Yatsenko, Metalware Scientific Research Institute, Beloretsk Metallurgy Combine, and Ukraine Special Steels Scientific Research Institute; UDC 621.771.25]

[Abstract] Researchers from the Metalware Scientific Research Institute worked together with researchers from the Ukraine Special Steels Scientific Research Institute and the Beloretsk Metallurgy Combine to develop a process for manufacturing extra-strong bolts from the steels 20, 20-PV, and 25 that have been heat-strengthened from rolling heating. Heat-strengthened carbon rod was produced by rolling in a single line on a 150 BMK mill. After leaving the mill, the steel rod was subjected to accelerated cooling (first in water to temperatures of 670-730° C and then in air to 500-550° C) on a wire-mesh conveyer. After heat-strengthening, the 7-, 8-, and 10-mm- diameter rods had a fine-grained ferrite structure (No. 9-10) and sections of perlite in amounts ranging from 15 to 45 percent. The rods had an ultimate breaking strength of 495 to 610 N/mm^2 and a Brinell hardness of 128-180. The metal was then sized on an AZTM 1/650 wire-drawing machine. AB 1918, AB 1919, and AB 1920 automatic machines were then used to cold-press the bolts. Tests performed on the bolts confirmed the fundamental possibility of producing bolts of class 8.8 strength from carbon rod that had been heat-strengthened by two-stage cooling and rolling heating. The study findings were then used to formulate specifications (TU 14-15-187-88) for 6.5- to 10-mm-diameter rod made from types 20 and 25 steel to be used for making strength class 8.8 bolts. Tests of the new process conducted at the Magnitogorsk Metalware-Metallurgy Plant indicated that introducing the new bolt-making process will result in significant cost savings. Table 1.

Modern Methods of Making High-Nitrogen Steels and Alloys and Outlook for Using Electroslag Arc Remelting Under Pressure for Their Production

937D0026A Kiev PROBLEMY SPETSIALNOY ELEKTROMETALLURGII in Russian
No 2 (30), Apr-May-Jun 92 pp 9-13

[Article by B.Ye. Paton, B.I. Medovar, V.Ya. Sayenko, Electric Welding Institute imeni Ye.O. Paton at the Ukrainian Academy of Sciences, Kiev; UDC 669.187.56.002.2]

[Abstract] The recent comeback of nitrogen and high-nitrogen steels and alloys due to the emergence of new applications and the discovery of new properties brought about by radical changes in steelmaking practices, e.g., a combination of high strength and ductility at liquid helium temperatures, prompted an investigation into the most promising high-nitrogen steel and alloy development trends since the first reports that Ni can be substituted with nitrogen and Cr-Ni stainless steels. The use of steels with a stable austenitic structure, alloyed with nitrogen, made by electroslag remelting (EShP) for cryogenic applications is reviewed, and a new method of

overcoming the nitrogen distribution irregularity by using a gaseous rather than solid-phase alloying addition is described. The new technology—electroslag arc remelting under pressure (DShPD) which is a combination of ESR and arc remelting under pressure (PDP)—whereby the electric arc burns between a consumable electrode and the slag bath surface using gaseous nitrogen ionized in the arc plasma is outlined in detail. It is speculated that the DShPD method will greatly improve the ingot's and wrought metal's nitrogen inhomogeneity. Attempts to reduce the level of steel contamination with impurities are summarized, and the experience of making Japanese cryogenic steels (JCS) is discussed. The importance of attaining high weldability of steels of a stable austenitic structure and the ability of producing welds with the same type of structure is stressed. It is suggested that metallurgy and welding experts combine their efforts in ensuring the highest quality of structures from high-nitrogen steels used for high-power fusion units. References: 1 Western.

Electroslag Arc Remelting of Titanium and Titanium Alloys

937D0026B Kiev PROBLEMY SPETSIALNOY ELEKTROMETALLURGII in Russian
No 2 (30), Apr-May-Jun 92 pp 13-15

[Article by B.I. Medovar, V.V. Shepelev, V.Ya. Sayenko, Yu.M. Pomarin, Electric Welding Institute imeni Ye.O. Paton at the Ukrainian Academy of Sciences, Kiev; UDC 669.187.56.002.3]

[Abstract] The increasing uses of titanium and titanium alloys in the other-than-aerospace industries under the on-going conversion policy and the possibility of lowering the metal cost due to the relaxation of the stringent military requirements prompted an examination of the titanium and titanium alloy electroslag remelting and vacuum arc remelting practices in Ukraine. It is noted that although a commercial ESR method was developed at the Paton Institute more than a quarter century ago, preference has been given to vacuum arc remelting, mostly for political reasons. The relative advantages and shortcomings of both methods are analyzed, and a new electroslag arc remelting method (DShP) developed at the Paton Institute, a combined process using two heat sources—electric arc and liquid conducting slag—is described. The new method is characterized by a higher remelted metal quality than ESR, a two- to threefold lower specific slag consumption, a 1.5 times higher electric power consumption, and the possibility of using direct or low-frequency alternating current. DShP ingots are distinguished by excellent macrostructure. It is speculated that the new practices will make Ti a common metal. It is stressed that electroslag arc remelting can and must be realized in conventional ESR furnaces by insulating the melting zone from the environment using the so-called flux gate. Figures 3; references 4.

How To Make Slab Ingots From Titanium and Its Alloys

937D0026C Kiev PROBLEMY SPETSIALNOY ELEKTROMETALLURGII in Russian
No 2 (30), Apr-May-Jun 92 pp 16-21

[Article by B.Ye. Paton, B.I. Medovar, V.Ya. Sayenko, A.G. Bogachenko, V.I. Us, A.V. Shepelev, Electric Welding Institute imeni Ye.O. Paton at the Ukrainian Academy of Sciences, Kiev; UDC 669.187.56.002.2]

[Abstract] The shortcomings of vacuum arc remelting (VDP) which makes it virtually impossible to produce slab-shaped ingots with a rectangular cross section and the difficulty of direct rolling of forging ingots into slabs or plates prompted an attempt to treat vacuum arc remelting as electroslag remelting and modify the process in order to adapt it to titanium and titanium alloys. To this end, the ingot spatial orientation is changed and the entire consumable electrode is positioned inside the mold, leaving only a small riser part outside the flux gate. Schematic diagrams of the new titanium alloy ESR technology capable of making up to 2.6 t ingots and a height of up to 400 mm in steel molds are cited. It is noted that the new flux gate ESR practices have the advantage of using compacted consumable electrodes from titanium sponge which is much cheaper than solid electrodes. The method is also capable of producing titanium slab ingots for subsequent rolling without billeting. It is speculated that the new ESR method for making titanium alloy slab ingots will find numerous applications for making cold- and hot-rolled plates and sheets for civilian purposes. Figures 5; references 7.

Electroslag Process Without Consumable Electrode Using Noncompact Filler Material

937D0026D Kiev PROBLEMY SPETSIALNOY ELEKTROMETALLURGII in Russian
No 2 (30), Apr-May-Jun 92 pp 27-32

[Article by Yu.M. Kuskov, Electric Welding Institute imeni Ye.O. Paton at the Ukrainian Academy of Sciences, Kiev; UDC 669.187.56.001.3]

[Abstract] The shortcomings of electroslag hard-facing due to the rigid constraints between the consumable electrode feed rate and the current and the need for different electrode sizes for each standard mold size prompted an attempt to use noncompact filler materials in electroslag surfacing and remelting; in ESR practices, these are often referred to as lump filler materials, microrefrigerators, or inoculants. A modification of this method developed at the Paton Institute is described in detail. In this case the consumable electrode is not used and the hard-surfacing or remelting process is carried out in the so-called current-lead mold (TPK) using noncompact filler materials. Schematic diagrams of three hard-surfacing and remelting methods in current-lead molds are cited and the mold design and operation are explained. The current-lead section is covered with a replaceable graphite lining in order to protect it from electrochemical erosion. The use of the current-lead molds for ESR makes it possible to utilize noncompact waste from

various processes, e.g., tool steel chips, and control the properties of the resulting metal within a broad range as well as develop new composites. The devices used for these practices are protected by patents in a number of countries. The ESR and electroslag hard surfacing device is a water-cooled mold consisting of several stacked sections. Ingot tests demonstrate the good serviceability of the chip remelting method. Figures 7; references 14.

On Possibility of Electroslag Remelting of Sulfurized Steel

937D0026E Kiev PROBLEMY SPETSIALNOY ELEKTROMETALLURGII in Russian No 2 (30), Apr-May-Jun 92 pp 32-34

[Article by V.V. Lakomskiy, Electric Welding Institute imeni Ye.O. Paton at the Ukrainian Academy of Sciences, Kiev; UDC 669.187.56.001.5]

[Abstract] Electroslag remelting is characterized by sulfur removal from the metal by the liquid slag; yet the need for sulfur-saturated free-cutting steel in order to improve machinability prompted a study of the possibility of using electroslag remelting of sulfurized steels while maintaining the sulfur content at the initial metal level. To this end, the sulfur behavior in the metal during electroslag remelting is investigated. An analysis of the sulfur removal reactions and the ability of slag to dissolve sulfur in the form of sulfides made it possible to suggest that basic fluxes be used and the metal and slag be deoxidized during the electroslag remelting of sulfur-saturated steels. It is also possible to blow an inert gas onto the slag bath surface in order to reduce oxygen's partial pressure. The high isotropic properties of sulfurized tool steel produced by electroslag remelting make it possible to eliminate subsequent thermoplastic deformation. References 9: 3 Russian, 6 Western.

Pilot Unit for Electroslag Arc Remelting of Ingots Weighing up to 0.5 Ton

937D0026F Kiev PROBLEMY SPETSIALNOY ELEKTROMETALLURGII in Russian No 2(30), Apr-May-Jun 92 pp 34-36

[Article by A.G. Bogachenko, V.Ya. Sayenko, V.A. Tikhonov, V.Ya. Maydannik, I.A. Lantsman, R.S. Dubinskiy, G.B. Shchupak, Electric Welding Institute imeni Ye.O. Paton at the Ukrainian Academy of Sciences, Kiev; UDC 669.187.56.001.3]

[Abstract] A lab unit designed and fabricated at the Paton Institute for electroslag arc remelting of ingots with a mass of up to 5 kg in an atmosphere of nitrogen at an up to 1 MPa pressure paved the way for the development of a pilot unit for making a 500 kg ingot in a mold with a 520 mm diameter in a nitrogen medium at an up to 1 MPa pressure. The design and operating principle of the DShDP-0.5 unit are described and its schematic diagram is cited. The principal elements of the ESR unit are an autoclave, a mold, and an ingot mold plate. The DShDP-0.5 unit specifications are summarized, and it is noted that a single-phase monofilar remelting principle is used. The consumable electrode is installed on the ingot mold plate and rolled under the head together with the plate, mold, and shell. Then the head is fastened to the consumable electrode and the cap is lowered until it is mated with the shell "flange to flange" and the flanges are fastened by a hoop. After that the actual ESR process takes place and the ingot is removed in the opposite sequence. Figures 1; tables 1.

Electron Beam Method of Coat Deposition on Composite Fibers

937D0026G Kiev PROBLEMY SPETSIALNOY ELEKTROMETALLURGII in Russian No 2 (30), Apr-May-Jun 92 pp 37-42

[Article by V.I. Ulyanov, A.F. Manulik, Ye.V. Onopriyenko, Electric Welding Institute imeni Ye.O. Paton at the Ukrainian Academy of Sciences, Kiev; UDC 669.187.526.001.5]

[Abstract] The lack of data on the possibilities of electron beam technology for making fiber-reinforced metallic composites due to the high cost and outlays for developing the necessary equipment prompted a study of the vacuum evaporation and condensation methods of making metal matrix composites. In particular, the possibilities of electron beam technology are considered for a single specific application: coat deposition on reinforcing fibers for metal matrix composites. To this end, a UE-173U lab electron beam unit equipped with three evaporation sources is used in an experiment carried out with two materials: high-strength stainless steel wire VNS-9 with a 0.15 mm diameter and boron fibers with a 0.14 mm diameter. The effect of the heating temperature on the fiber strength is plotted. To protect the fibers from chemical interaction with the matrix material, it is coated with a 0.8-10 μm TiB_2 layer applied on top of an aluminum-based adhesive sublayer. In addition, ZrO_2, NbC, TiC, and ZrB_2 coats are tested. The procedure of applying the matrix material over the protective coat is outlined. The issue of the low ductility of intermetallic compounds is addressed, and it is suggested that this problem be solved by using these compounds as the reinforcing fibers. Applications of microlayer laminated composites produced by electron beam deposition are discussed, and it is noted that a number of laminated composites have superplasticity and can replicate the properties of Damascus steel. Figures 6; references 10: 7 Russian, 3 Western.

Substructural Hardening of Pure Polycrystalline Nickel

937D0026I Kiev PROBLEMY SPETSIALNOY ELEKTROMETALLURGII in Russian No 2 (30), Apr-May-Jun 92 pp 53-60

[Article by T.A. Molodkina; UDC 669.187.526.001.5]

[Abstract] The use of substructural hardening, i.e., accumulation, interaction, and subsequent reordering of dislocations during plastic deformation with the formation of a cellular or polygonal structure or substructure, for

increasing the metal strength whereby the topography of the future substructure is determined by the grain boundaries and their extent is discussed. An equation is derived for determining the effect of the grain dimension on the flow stress. The strain hardening curves in true and differential coordinates, the dependence of the microscopic yield strength on the straining degree, the dependence of the flow stress on the grain size at various straining degrees, the dependence of the lattice friction stress and Hall-Patch coefficient on the straining degree, the dependence of the flow stress on the mean cell size for various grain sizes, and the dependence of the mean cell size on the dislocation density are plotted. Straining is performed in an Instron machine by uniaxial tension, and the structure is examined under a JSEM-200 electron microscope. An analysis demonstrates that that the straining curves plotted in differential coordinates clearly reflect process stages whereby each strain hardening stage corresponds to its own predominant structure: stage I is characterized by a uniform dislocation distribution, stage II—by a cellular structure with a small constant disorder angle, and stage III—by a fragmented structure with a disorder angle of 0.5 to 5°. The flow stress under straining which facilitates the cellular structure formation is inversely proportionate to the cell size; at a strain exceeding 16 percent, the mean disorder angle of the resulting substructure increases due to the fragmented structure development. Figures 6; references 16: 5 Russian, 11 Western.

Electrovacuum Liquid Steel Ladle Refining Method

937D0026J Kiev PROBLEMY SPETSIALNOY ELEKTROMETALLURGII in Russian
No 2 (30), Apr-May-Jun 92 pp 97-101

[Article by V.G. Ivanov, N.A. Kravchenko, V.T. Tereshchenko, M.I. Gasik, Dnepropetrovsk Metallurgical Institute and Tulachermet Scientific Production Association of Ferrous Metallurgy; UDC 669.187.2]

[Abstract] The shortcomings of ladle refining of steel in DH or RH units which combine electric arc heating and subsequent liquid metal degassing at a low residual pressure, such as the low heating rate of under 2-5° C/min and disruptions in the steelmaking process due to differences in the duration of various stages as well as the need to use scarce graphitized high-quality electrodes and metal carburization prompted the Electrometallurgy Department at the Dnepropetrovsk Metallurgical Institute (DMetI) to develop a new method of ladle refining of steel. The new method referred to as the electrovacuum steel refining (EVS-DMetI) amounts to tapping the semifinished liquid steel from an arc furnace or oxygen converter into a ladle without any additional reheating, then degassing the ladle and igniting an electric arc discharge over the metal surface by passing current through the metal jet. The method makes it possible to accelerate the refining process and shorten the ladle treatment duration by 30-50 percent by combining the metal heating and degassing operations. The heating rate reaches 10-20K/min which is 3-5 times higher than that of conventional procedures while the liquid metal jet plays the role of a plasma generator. The proposed method is recommended for commercial implementation. Figures 2; tables 1; references 9: 6 Russian, 3 Western.

Laser Treatment of Titanium Surface and Titanium Alloys in Nitrogen Atmosphere

937D0026K Kiev PROBLEMY SPETSIALNOY ELEKTROMETALLURGII in Russian
No 2 (30), Apr-Jun 92 pp 102-105

[Article by Yu.M. Pomarin, V.Yu. Orlovskiy, B.I. Medovar, O.A. Velichko, G.M. Grigorenko, V.Ya. Sayenko, S.R. Gurgu, Electric Welding Institute imeni Ye.O. Paton at the Ukrainian Academy of Sciences, Kiev; UDC 669.187.2]

[Abstract] The unique combination of physical, chemical, and mechanical properties of Ti and its alloys whose surface is saturated with nitrogen and the shortcomings of known nitriding methods, i.e. the formation of a thin, hard, and brittle titanium nitride layer and the need for extended heating at a high temperature, prompted an investigation into laser treatment of Ti and titanium alloy surfaces in an atmosphere of nitrogen. To this end, laser fusing of the surface is examined in detail since fusing is known to be the best nitriding technique. The microhardness of the titanium and alloy surface treated with a laser beam is summarized, and the dependence of the surface layer microhardness on the fusing rate and depth and the nitrogen content and the dependence of the nitrogen concentration in the surface layer on its fusing rate at a varying laser beam power are plotted. Tests show that the nitrogen concentration in the surface layer largely depends on the treatment rate and less so on the laser beam power. The study demonstrates the possibility of making titanium and titanium alloy products which combine high strength properties of the surface layer with a specified fusion depth and a high base ductility. Figures 5; tables 1; references 4: 3 Russian, 1 Western.

Tool Steel Production by Electroslag Remelting

937D0026L Kiev PROBLEMY SPETSIALNOY ELEKTROMETALLURGII in Russian
No 2 (30), Apr-Jun 92 p 113

[Article by I.V. Galotok]

[Abstract] The use of electroslag remelting for making high-quality tool steel with a high homogeneity, isotropism, and purity is discussed, and it is noted that despite the tendency of the ESR process to remove sulfur from steel, it can be used for making sulfur-alloyed steel by using slags with a specific composition. The advantages of the ESR method are outlined and the effect of ESR on the microstructure and properties of tool steel ingots from high-speed steel S6-5-2 and die steel X40CrMoV51

and X38CrMoV51 (examined by the Thyssen Edelstahlwerke AG company) is summarized. The study shows that sulfur-alloyed steels with 0.1 percent S have a highly disperse and isotropic structure making it possible to avoid subsequent heat treatment and improve machinability. It is asserted that despite the added cost compared to conventional smelting, ESR is effective for making both desulfurized and sulfurized steels. References: 1 Western.

Coat Formation Process Activation

937D0031F Moscow IZVESTIYA VYSSHIKH UCHEBNYKH ZAVEDENIY: CHERNAYA METALLURGIYA in Russian No 2, Feb 92 pp 39-40

[Article by N.I. Ivanov, A.V. Vachayev, Magnitogorsk Mining and Metallurgical Institute; UDC 669.18:620.198:(539+534-08)]

[Abstract] The role of temperature conditions in enhancing the formation of coats, especially high-temperature refractory coats, and the development of crystal structures are discussed, and it is noted that the crystal properties may be used to intensify the coat formation process. If the crystalline formation is treated as an entity possessing a certain energy typical of all ordered systems, this energy is partially represented by the vibrational energy of the developing crystal lattice. The equation of the crystal lattice cell vibrations under an external force, i.e., a linear resonance equation, is derived and analyzed and the onset of linear resonance described by Duffing's equation is solved. A model of the coat and base material interaction when vibrations are excited in the base in a subresonance mode is developed. The outcome of an experiment to apply water, BF-6 glue, nitrocellulose enamel, and paraffin coat materials to the surface of steel St3 in which ultrasonic vibrations are excited at a 70 kHz frequency and a 7 W/cm^2 intensity are summarized; the findings are consistent with the model and show that ultrasonic treatment facilitates the development of better coats except for paraffin which crumbles and comes off. It is noted that a combination of thermodynamic and vibrational factors during the coat formation has a favorable effect on the process and makes it possible to obtain high-quality products. Tables 1; references 3.

Austenitic Structure Behavior Characteristics of Hypo- and Hypereutectoid Steels Under Surface Layer Treatment With Electric Arc

937D0031G Moscow IZVESTIYA VYSSHIKH UCHEBNYKH ZAVEDENIY: CHERNAYA METALLURGIYA in Russian No 2, Feb 92 pp 46-49

[Article by N.N. Davydova, V.N. Davydov, Urals Polytechnic Institute; UDC 669.046:621.785.5]

[Abstract] The effect of the austenite grain on the developing structure during heat treatment of steel and the range of mechanical properties of steel products is discussed, and an attempt is made to trace the behavior patterns of the austenitic structure as a function of the electric arc hardening conditions. To this end, metallographic studies are carried out in steel 45KhNM and 150 KhNM using Neophot-2 and Epiquant microscopes after etching the hardened layers in a 4 percent nitric acid solution in alcohol. The samples were surface hardened both with and without beam scanning. The hardening conditions are summarized, and the grain size distribution in steel 45KhNM with an original martensitic structure without scanning and on steel 150KhNM with scanning are plotted. The effect of the original structure changes on the hardened layer formation is noted and the carbide phase precipitation from the martensite structure is examined. The study revels the possibility of greatly refining the austenite grain under electric arc hardening with and without the beam scanning. Scanning makes it possible further to refine the grain and equalize the size through the depth due to thermal cycling. By manipulating the arc current and energy source movement one can control the grain size and the size differential parameter throughout the hardened zone. The surface hardening technology has been implemented at the Nizhniy Tagil Integrated Iron and Steel Works. Figures 3; tables 1; references 2.

Metastable Liquid Alloy Microstratification and Its Effect on Casting Structure

[Article by A.S. Popel, Urals State Teachers College; UDC 621.745.01]

[Abstract] The experience accumulated in metallurgical practices which attests to the fact that given the same chemical composition, the structure and properties of alloys largely depend on the type of the charge materials used and the methods of their addition to the system is summarized on the basis of numerous published sources. The structural metallurgical heredity phenomenon, whereby the set of such characteristics as the volume fraction of carbides in the initial pig iron and its effect on the casting properties, the effect of the fine-grain pig iron and scrap metal structure on the structure and properties of open hearth steel, and the effect of the electrode wire on the weld properties, transfer the charge peculiarities to the casting through the liquid state is discussed. The hereditary nature of microstratification of liquid eutectics is examined in detail; the microseparation of Sn-Pb alloys into layers, the temperature dependence the Sn-Pb alloy density, and the domains of metastable microheterogeneity of binary alloys are plotted. An analysis of the microstratification domains in various alloys shows that their temperature-concentration extent depends on the reciprocal solubility of the components in the solid state. The inherited microheterogeneity of binary alloys dissolves fully under equilibration; the metastable microheterogeneity breakdown temperature depends not only on the main component concentration but also on the impurity concentration in the melt and phase dispersion in the initial sample's crystalline structure. The study

established that colloidal particles probably serve as the principal "genes" of metallurgical heredity which are responsible for transmitting the structural characteristics of the charge to the ingot or casting through the liquid state. Experimental data attesting to the efficiency of this mechanism will be considered in the next report. Figures 3; references 17.

Spin Casting of Thin-Walled Aluminum Alloy Parts

937D0036D Moscow LITEYNOYE PROIZVODSTVO in Russian No 7, Jul 92 pp 16-17

[Article by Z.A. Vasilenko, G.G. Krushenko, B.A. Balashov, A.N. Timofeyev, L.G. Ladnyuk, Data Center at the Siberian Department of Russia's Academy of Sciences and Krasnoyarsk Aluminum Smeltery; UDC 621.74.042:669.715]

[Abstract] The high cost of die casting (LPD) and the urgency of using cheaper secondary alloys for making thin-walled aluminum alloy castings prompted the development of a small spin casting unit with a vertical axis for this purpose which can be easily placed at any location in the foundry. The casting process steps are outlined in detail and the cross section of a boat screw propeller casting made by this method is shown for illustration. The properties of the primary alloy AL9 and secondary alloy AK5M2 are compared and the dependence of the properties of the AK5M2 alloy on the pouring method and blade section position is plotted. Corrosion tests show that both alloys have virtually the same corrosion resistance and electrochemical characteristics while the surface quality of the AK5M2 casting is better. An analysis demonstrates that substitution of the primary alloy with the secondary alloy in spin casting and the resulting 23 percent reduction in metal outlays per casting due to a decrease in the discard head volume and a reduction in the machining labor outlays lead to an annual saving of close to 50,000 rubles. Figures 2; references 5.

Characteristics of Composite Metal Pipe Spin Casting

937D0036E Moscow LITEYNOYE PROIZVODSTVO in Russian No 7, Jul 92 pp 17-18

[Article by G.D. Novruzov, F.A. Nadzhafzade, Z.G. Iskenderov, Azeri Engineering University and Machine Building Plant imeni Lieutenant Schmidt; UDC 621.74.042]

[Abstract] The low practicability and brittleness of ferrosilide used for making corrosion resistant steel prompted an experiment with spin casting of composite metal pipes with consecutive metal layer pouring. To this end, the SCh 15 grey pig iron and SI15 ferrosilide are used; cast iron is smelted in a cupola and ferrosilide—in an induction furnace with an acid lining, and the pipes are cast in a centrifugal Lipetsk unit in hot molds with a heat insulating coat. The spin casting procedure is outlined in detail. An analysis of pilot castings with a 4-5 mm inner ferrosilide layer shows that a nonuniform structure forms throughout the casting wall, depending on the chemical composition, casting temperature, cooling rate, and other casting parameters. The behavior of the Si, C, and graphite concentration in the transition zone thickness of the clad metal casting is plotted. It is shown that the best layer binding is attained at an optimum time interval (IV) between the start of the pig iron and ferrosilide casting. The optimum time interval is 45-60 seconds. The conclusion is drawn that the method of successive spin casting into a rotating mold makes it possible to control the casting quality and properties within the optimum time interval. Figures 1; references 1.

Casting Molds for Making Titanium Castings

937D0036F Moscow LITEYNOYE PROIZVODSTVO in Russian No 7, Jul 92 pp 19-21

[Article by V.A. Chernikov, G.L. Khodorovskiy, V.N. Larionov, Ye.N. Khlystov, Saturn Scientific Production Association and Scientific Research Institute of Aviation Engineering; UDC 621.74.045:669.295]

[Abstract] The lack of available and cheap molding materials which ensure the necessary quality of cast titanium products in an environmentally clean process necessitated the development of a composite mold, e.g., from a silicon dioxide or a more refractory oxide containing SiO_2 as a binder. To investigate the effect of SiO_2 on the quality of Ti castings, synthetic corundum molds with a binder on the basis of the ETS-40 material containing 2.5-18 percent SiO_2 and 10 percent of ASD-4 Al powder are made and filled with the VT20L alloy by spin casting method in a UPKhT-2 unit, then samples are cut from the casting for testing. An increase in the altered layer thickness with the wall thickness is observed, and the dependence of the altered casting layer depth and noncalcinated ceramic mold strength on the SiO_2 content in the binder, the SiO_2 distribution in the aluminum oxide mold layer as a function of the SiO_2 content in the binder, and the surface microhardness behavior in the casting cross section are plotted. The study reveals that a decrease in the silicon dioxide concentration leads to the altered layer depth decrease and a reduction in the ceramic mold strength, and it shows that the latter can be compensated for by increasing the calcination temperature and adding a finely disperse thermodynamically stable powder to the composition. The SiO_2 distribution is nonuniform due to its migration toward the mold surface. The expediency of using combined ceramic molds with a retarding layer or several layers which prevent the SiO_2 migration is suggested. Figures 3.

Sodium Silicate Solution Core Sands for Making Bladed Impeller Castings

937D0036H Moscow LITEYNOYE PROIZVODSTVO in Russian No 7, Jul 92 p 33

[Article by S.F. Nagibin, B.I. Sych, Sumy Tsentrolit Cast Iron Foundry and Kharkov Polytechnic Institute; UDC 621.743.49]

[Abstract] A special core sand on the basis of water glass developed at the Sumy Tsentrolit Pig Iron Foundry and implemented for making impeller castings from grey cast iron is described. The necessary physical, mechanical, and handling properties of the core sand are attained by using a ShOS complex additive—a shale byproduct—and a high-refractory additive, such as kaolin. The chemical composition of the core sand and its physical and mechanical properties are summarized. The sand knockability is estimated by the method developed at the Central Scientific Research Institute of Machine Building. The use of the sand made it possible to decrease casting rejection due to hot crack, expansion scabs, and burnt-on sand and lower the casting cost. Tables 2.

Cast Metal Matrix Composites

937D0037A Moscow LITEYNOYE PROIZVODSTVO in Russian No 8, Aug 92 pp 3-4

[Article by I.V. Gavrilin, Vladimir Polytechnic Institute; UDC 621.746.6]

[Abstract] The developments in the field of cast composites (LKM) in the CIS and United States are compared, and the work being performed at the MIT, University of Wisconsin, General Motors, Control Data Corporation, and Naval Research Center in the United States and Institute of Mechanics, Technology, and Materials in Vladimir, IPL casting institute at the Ukrainian Academy of Sciences, Moscow Steel and Alloy Institute, and other organizations in the CIS is described. The cast composite production technology and reinforcing cast composite phases and an increase in the number of publications on this subject in 1980-1991 are summarized. The differences in the efforts being undertaken in the United States and CIS are outlined, and the need to integrate research programs is stressed. Ongoing studies are classified by the goals, scientific peculiarities, production methods, cast composite compositions, development forecasts, cast composite properties, economic indicators, and cooperation. The similarity in the methods of cast composite production is responsible for the similarity of scientific approaches while the differences can still be useful and may and must become a source of new development concepts. Tables 2.

Experimental Measurement of Chronal Properties of Materials

937D0037B Moscow LITEYNOYE PROIZVODSTVO in Russian No 8, Aug 92 pp 8-12

[Article by A.I. Veynik, S.F. Komlik, Engineering Physics Institute at the Belarussian Academy of Sciences; UDC 621.74.08]

[Abstract] The importance of knowing the quantitative characteristics and properties of the chronal phenomenon contained in the equations of the seven principles of the general theory (OT)—a *sine qua non* of engineering analyses is stressed, and these properties are identified as the chronal charge (or the chronor), the chronal (or the chronal analogue of the squared velocity, rotation speed and vibration frequency, temperature, electric potential, pressure, etc.) and chronocapacity, chronoconductivity, chronotransfer coefficient, etc., as well as the mass (or the metrior) and squared velocity (or the metrial). The design of an experimental unit for determining the chronophysical properties of substances using a chronal accumulator (a piece of sugar) and a magnetic amplifier is described, and the chronal distribution along the sample is plotted. Schematic diagrams of an experimental unit using cosmic chronal radiation and a unit for determining the force of interaction between chronally charged batches are cited. The frequency behavior during the tests of a pine sample with positively charged sugar as the source of chrones, the frequency behavior at the chronal flux input and output, and the frequency behavior during tests of a copper sample are plotted. The importance of exercising extreme care in chronal experiments so as not to harm one's health is stressed, and a strict warning is given against mass "healing" of TV and radio listeners and viewers and live audiences; it is speculated that the chronal phenomenon has a tremendous potential for science, engineering, medicine, agriculture, etc. Figures 6; tables 1; references 3.

Die Casting Development Tasks

937D0037D Moscow LITEYNOYE PROIZVODSTVO in Russian No 8, Aug 92 pp 16-17

[Article by M.L. Zaslavskiy, R.A. Korotkov, Yu.F. Ignatenko; UDC 621.74.043]

[Abstract] A trend toward an increasingly large proportion of die cast products and the large number of patens in the field of die casting (LPD) prompted a reevaluation of the die casting development tasks; it is noted that the casting machine design is the primary factor ensuring correct die casting process. The capabilities of die casting machines developed by the Siberian Casting Machine Association and other organizations are discussed, and the possibilities of expanding die casting applications and automating the process with the help of computers are outlined. The use of automatic temperature control

devices produced at Minsk, Smolensk, Volgograd, Yekaterinburg, Odessa, Novosibirsk, and Zaporozhye enterprises is described, and it is noted that all machined exhibited at the GIFA international fair are equipped with either self-contained or semiautonomous mold temperature controllers. The effect of the cast part design on the casting strength and density and new trends toward using composites with ceramic reinforcement are discussed. Work on developing new die casting machines with a high backpressure using existing defense technologies is mentioned. The importance of automating all stages of the die casting process and developing flexible production modules (GPM) is stressed, and the conclusion is drawn that the future of die casting lies in developing production processes and equipment on the basis of computer-aided process control systems (ASUTP) and improving the management practices of die casting foundries on the basis of automatic control systems.

Robotized Complex for Making Foundry Investment Patterns

937D0037E Moscow LITEYNOYE PROIZVODSTVO in Russian No 8, Aug 92 pp 18-19

[Article by I.B. Sokol, V.M. Belyayev, L.G. Budanova, Scientific Production Association of the Scientific Research Institute of Automotive Engineering Industry; UDC 621.74.045]

[Abstract] The increasing use of industrial robots (PR) in investment casting (LVM) foundries in the United States, Great Britain, Canada, Japan, and other industrialized countries vs. a sole example of industrial robot use in Russia is mentioned, and the urgency of using industrial robots in foundries making agricultural machinery is emphasized. It is noted that attempts to develop robotized complexes (KR) at a number of domestic enterprises have been unsuccessful, largely due to the difficulty of industrial robot production. A robotized complex whose production is developed at the Volga Automotive Plant (VAZ) Production Association is described, and its schematic diagrams are cited; the absence of rigid constraints and the possibility of programming the robotized complex make it easy to adapt it to a specific production room or a range of castings in existing foundries. The specifications of the robotized industrial complex for making investment patterns are summarized and its principal operating positions are shown. Figures 5; tables 1.

Investment Casting Shop for Multiple Item Production

937D0037F Moscow LITEYNOYE PROIZVODSTVO in Russian No 8, Aug 92 pp 20-21

[Article by V.G. Puchkov, Donets Central Design Office, Lugansk; UDC 621.74.045]

[Abstract] Commissioning of an investment casting foundry shop with a $\leq$200 t/year capacity necessitated changes in the production bay layout and an addition of an extra fettling building. A plan view of the investment molding shop and ancillary bays is shown. A large amount of finely disperse air is mixed in with the investment pattern sand in order to eliminate shrinkage and improve the pattern investment quality, making it possible to develop "foam patterns" while the use of filling risers made it possible not only to increase the labor productivity, but also eliminate cracking during melting out of the investment pattern. The use of a ready binder in molding the refractory coat makes it possible to eliminate the hydrolysis operation and stabilize the process. The developer of the investment molding shop is offering technical assistance in setting up similar operations. Figures 1.

Models of Complex Effect of Postexplosion Steel + Bronze Composite Treatment Conditions on Joint Strength

937D0029A Moscow IZVESTIYA VYSSHIKH UCHEBNYKH ZAVEDENIY: CHERNAYA METALLURGIYA in Russian No 4, Apr 92 pp 32-34

[Article by Ha Min Hung, Ye.U. Atabekov, Moscow Steel and Alloy Institute; UDC 621.791.13+621.771]

[Abstract] The need to develop a mathematical model for selecting the process parameters of explosion joining and subsequent rolling and heat treatment and for controlling them prompted the development of a 3^3 experiment design according to the following complex of variables: the heating temperature, exposure duration, relative deformation, and cooling rate. The tearing strength of a composite made from steel 08kp + bronze Br6.5-0.15 as a function of the temperature, exposure, and relative deformation and the joint strength of this composite as a function of the temperature, cooling rate, and relative deformation found by mechanical tests of ring samples and statistical processing of experimental data are summarized. The dependence of the layer tearing strength of the explosion-made composite on the subsequent rolling and heat treatment conditions is plotted, and mathematical models of the effect of process parameters as well as computer analysis results produced on the basis of these models are presented. The findings point to the fact that rolling and heat treatment lead to a loss of strength, recrystallization, and formation of new phases and chemical reactions between the components. Each process may become dominant under a certain combination of conditions; the intensity of these processes, as a rule, increases with temperature. This leads to the conclusion that the composite's properties can be controlled by manipulating the parameters; by using the mathematical model, one can specify the optimum heat treatment and rolling conditions with sufficient precision for ensuring a high quality of composite layered sheets for making plain bearings. Figures 1; tables 2; references 3.

Behavior of Mechanical Properties of Steel Kh18N10T Wire After Electrically Stimulated Drawing

937D0029G Moscow IZVESTIYA VYSSHIKH UCHEBNYKH ZAVEDENIY: CHERNAYA METALLURGIYA in Russian No 4, Apr 92 p 81

[Article by O.V. Aponasenkova, V.Ya. Tsellermayer, V.Ye. Gromov, Siberian Metallurgical Institute and Strength Physics and Materials Science Institute at the Siberian Department of the USSR Academy of Sciences, Tomsk; UDC 669.14.018:539.4.015]

[Abstract] Interest in the process of plastic deformation under external energy factors, such as pulse electric currents, is noted, and an attempt is made to determine the mechanism of the effect of pulse current on the structure and mechanical properties of austenitic steel. To this end, wire from polycrystalline stainless steel Kh18N10T subjected to traditional and electrostimulated drawing at a 1.88 m/s rate with a total reduction of up to 57.4 percent after ten passes at a current density of 1,200 MA/m^2 at a 200 Hz frequency is examined. The surface temperature during the drawing does not exceed 200° C. The dislocation structure of steel after regular drawing at a 13 percent reduction and electrostimulated drawing at a 44 percent reduction is shown at a 50,000 magnification, and the comparative behavior of the ultimate strength and other mechanical properties is summarized. The study shows that the dislocation structure evolves by a mechanism typical of single-phase FCC alloys with a mean packing energy: chaotic dislocation distribution → knotted structure → cellular structure + twinning → striped disoriented structure → fragmented structure. The conclusion is drawn that electrostimulated drawing leads to the appearance of recrystallization twins, i.e., recovery substructures, due to localized heating by the pulse current which probably causes a dynamic recovery, partial stress relaxation, and, as a consequence, an increase in ductility. This strain mechanism is confirmed by a twin expansion under the same reduction degree. Figures 1; tables 1; references 5.

Determining Permissible Blooming Mill Rolling Rate According to Stability Criterion

937D0031E Moscow IZVESTIYA VYSSHIKH UCHEBNYKH ZAVEDENIY: CHERNAYA METALLURGIYA in Russian No 2, Feb 92 pp 25-27

[Article by V.M. Klimenko, A.V. Svetlichnyy, Donetsk Polytechnic Institute; UDC 621.771.22]

[Abstract] The issue of determining the maximum permissible blooming mill rolling rate from the viewpoint of avoiding slippage which is accompanied by considerable dynamic loads and leads to an accelerated equipment wear and breakage is addressed, and analytical formulae are derived on the basis of known data for determining the maximum permissible rolling rate under the specific conditions and a given reduction diagram. The dependence of the arm of moment on the shape of the form factor of the deformation focus during rolling on barrel-shaped and cylindrical rolls and in the pass and permissible values of the maximum rolling rate are plotted. The kinematic parameters of the rolling of a 5.6 t ingot in a blooming mill are summarized. The maximum steady-state blooming mill rolling rate (i.e., the upper bound of the feasible range) depends on the ingot material and the roll surface state, the type and temperature of ingot steel, the form factor of the straining focus, and the degree of the rolling pass filling with the metal. It is noted that the actual rolling rate within the feasible range should be selected on the basis of standard criteria. Figures 3; tables 1; references 2.

Methods of Cast Iron Production for Engine Valve Seats

937D0037C Moscow LITEYNOYE PROIZVODSTVO in Russian No 8, Aug 92 pp 6-8

[Article by V.M. Grabovyy, G.I. Slynko, I.P. Volchok, Melitopol Engine Works; UDC 621.74.002.6:669.15]

[Abstract] Excessive valve seat wear in today's internal combustion engines (DVS) due the plastic displacement of the bevel material at a high temperature under static and dynamic loads is noted, and the criteria which determine the valve seat serviceability are formulated: heat resistance, straining ability, and wear resistance which depends on the material's hardness. Production practices of making engine valve seats from high-alloy and low-alloy grey pig iron are outlined, and the chemical composition of these cast irons brands is discussed. In particular, the use of alloyed phosphorous pig iron for making valve seats for the MeMZ-245 engine of the ZAZ-1102 vehicle at the Melitopol Engine Works (MeMZ) is described in detail, and the results of laboratory and commercial tests of the engine valve seats are presented. The optimum correlation of the Cr and P alloying additions and the joint effect of the Si, Cr, Mo, Mn, Ni, and Cu alloying elements on the heat resistance of phosphorous pig iron are established and a mathematical experiment design is formulated. Data of a quantitative point analysis carried put in a Camebax unit indicate that the Mo and Cr concentration in the metal matrix is high despite their distribution patterns. The operating experience of valve seats in 1988-1991 shows that the wear of engine valves from cast iron 360S3KhGMD in MeMZ-245 engines does not exceed that of Cr-Ni white cast iron 290S2Kh14GN9 and is lower than the wear in MeMZ-968 engine by fourfold. Implementation of the phosphorous cast iron production practices lowered the production cost of 1 t of valve seat castings by 10 percent compared to Cr-Ni white cast iron, decreased labor intensity by 4.5 times, increased the valve seat strength, and reduced the number of rejects. References 4.

Heat Conditions of a Monolithic Tantalum Capacitor Undergoing Infrared Soldering

927D0250A Kiev AVTOMATICHESKAYA SVARKA in Russian No 3, Mar 92 pp 26-30

[Article by N. M. Fialko, V. G. Sarioglo, N. Chebanova, Institute of Engineering Thermophysics, Ukrainian Academy of Sciences, V. G. Prokopov, Kiev Polytechnical Institute, and A. A. Grachev, Scientific Research Institute of Special Electronic Machine Building, Kiev; UDC [621.791.35:66.085.1]:669.294:621.319.4.002]

[Abstract] Mathematical modeling was used to investigate heat transfer processes in infrared soldering of a monolithic tantalum capacitor to a ceramic printed circuit board. In this operation, the selection of process parameters involves the need to maintain heat conditions in the printed board assembly, which meet certain requirements. The first requirement is for the maximum temperature of the solder to fall within certain limits defined by the melting point of the solder and the required levels of its superheating. Secondly, the temperature of the printed board assembly as a whole must not exceed a certain permissible level. The last requirement is associated with limiting the rate of the assembly's heating in the soldering process.

In the light of these requirements, the heat conditions of the printed board assembly were analyzed, and the relationship between such process parameters as the rate of movement of the furnace conveyor and the necessary temperature of the IR heater was determined. For rates of movement of 3, 4.5, and 6 millimeters per second, the necessary temperatures were determined to be 265, 315, and 350° C, respectively.

Properties of Plate and Welds Made of the Nitrogen Steel 03Kh2ON16AG6

927D0250B Kiev AVTOMATICHESKAYA SVARKA in Russian No 3, Mar 92 pp 31-34

[Article by K. A. Yushchenko, L. V. Chekotilo and G. G. Monko; Institute of Electric Welding, Ukrainian Academy of Sciences, O. G. Filatov, Scientific Research Institute of Electrophysical Apparatus, and Yu. G. Gabuyev, "Dneprospetsstal" Plant, Zaporozhye; UDC 621.791.052:669.15-194-415]

[Abstract] New products made of 03Kh2ON16AG6 steel, which contains 0.20-0.30 percent nitrogen, for use in magnetohydrodynamic generators, cryogenic generators, fusion energy installations, and other special equipment are reviewed. The products are made by open arc melting and electroslag remelting. They include: plates 40, 60, 70 and 90 mm thick; 3000, 2500 and 1550 mm wide; and 6800-9000 mm long and slabs 140, 190, 300 and 450 mm thick; 615, 740, 1230 and 1750 mm wide, and 4800, 5000, 3800 and 2600 mm long; flanged hollow and solid cylindrical forgings 300-620 mm in diameter with wall thicknesses of 80-220 mm and weighing up to two tons; and round billets 200 mm in diameter and weighing 600-700 kg. Also, new technology has been introduced for melting 03Kh2ON16AG6-GR steel in an arc furnace and refining it to the required chemical composition in an oxygen steelmaking furnace. Plates and slabs of these steels can be used to make key assemblies of new equipment operating at very low temperatures. For example, plates and slabs 90 and 220 mm thick were used in the coil of a superconductive magnet of a 100,000 kW magnetohydrodynamic generator. Electroslag remelting substantially increases the steel's purity and the ductility and stability of mechanical properties of plates and slabs. Technology also has been developed for electroslag welding of plates, slabs, and shells of all thicknesses made of these steels.

Tables are given showing the mechanical properties of plate of various thicknesses made of the steels and the amount of inclusions in plate after electroslag remelting.

Electron-Beam Welding of Heat Exchangers Made of Aluminum Alloys

927D0250F Kiev AVTOMATICHESKAYA SVARKA in Russian No 3, Mar 92 pp 53-54

[Article by A. A. Bondarev and S. V. Nazarenko, Institute of Electric Welding, Ukrainian Academy of Sciences, and I. I. Dyakov and B. Ye. Pyshkin, Belarus Polytechnical Institute; UDC 621.791.72:621.565.93/.94:669.715]

[Abstract] The Institute of Electric Welding has developed an environmentally clean, waste-free technology for manufacturing highly effective ribbed heat exchangers from aluminum alloys for use in motor vehicles and tractors, heat power installations, refrigeration equipment, etc. Multichannel ribbed heat-exchanger elements are welded to tube plates using an electron beam, which makes welds uniformly strong, with a high density and completely free of deformations. The heat-exchanger elements are made in round or flat multichannel sections according to a waste-free technology developed at the Belarus Polytechnical Institute. Depending on the characteristics of the heat exchanger, ribs can be made as high as 20 mm with tabs ranging in thickness 0.1-0.7 mm. Welding of each heat-exchanger element to the tube plate is accomplished in one pass, with the beam program-controlled and with application of heat to edges of the element regulated according to its thickness and weight. In comparison with brass or copper heat exchangers, in which ribs are made using foil soldered to tubes, welded heat exchangers made of aluminum alloys are only one-fourth to one-third as heavy and have 20-40 percent better heat-exchange performance.

Variation in Mechanical Properties of 110G13L Steel as a Result of High-Temperature Heating

927D0250G Kiev AVTOMATICHESKAYA SVARKA in Russian No 3, Mar 92 pp 54-55

[Article by A. V. Yakimov, Tashkent Institute of Railroad Transportation Engineers, and S. N. Kiselev, Moscow Institute of Railroad Transportation Engineers; UDC 621.791.927.042:669.15'74- 194]

[Abstract] Variation in the tensile strength and necking down of specimens of high-manganese 110G13L steel as a result of high-temperature heating was investigated. The ductile-to-brittle transition temperature range for this steel was determined to be 900-1300° C. It was demonstrated that a possible cause of reduced ductility is the formation of a film of poorly wettable phosphorus-containing phases (probably of eutectic composition) along boundaries of austenitic grains. This weakens the bond between grains and leads to failure of high-manganese steel. Accumulations of phosphorus in boundary zones of grains form during crystallization of castings due to the poor solubility of phosphorus in high-manganese austenite, and they are not eliminated during subsequent heat treatment. Therefore, a sharp drop in ductility at temperatures above 900° C is typical for industrial grades of 110G13L steel containing up to 0.1 percent phosphorus.

Recovery of Wastewaters of Na-Cationite Filters

937D0003G Moscow STAL in Russian No 7, Jul 92 pp 89-90

[Article by L.N. Poletayev, A.S. Sobol, and I.V. Pushel, Zaineftekhim, PTP Tsentroenergochermet [not further identified], and Belarus Department, All-Union Scientific Research and Design Institute of the Power Industry; UDC 621.187.12]

[Abstract] Na-cationite filters are widely used in industry to remove Ca^{2+} and Mg^{2+} cations from water. Significant amounts of wastewaters are generated when the cation exchangers are regenerated. Ion-exchange technologies are one way of protecting reservoirs from becoming contaminated with spent mineralized solutions from Na-cationite filter-based water-softening processes. The authors of this article have examined two versions of a method for recovering spent solutions of Na-cationite filters. The wastes generated by the first version of the recovery methods are in the form of a complex fertilizer, whereas those generated by the second version are uniform solid sediments that may be used as substitutes for various chemical products. According to version one of the new method, the spent solution passes from the Na-cationite filter to a settling tank, where the hardness ions are treated with a 10 percent Na_3PO_4 solution for six hours. The treated solution has a residual hardness of 50 mg-equivalent/liter and a residual phosphate concentration of 1.0 to 1.5 mg-equivalent/liter. The condensed sediment, which is a mixture of $Ca_3(PO_4)_2$ and $Mg_3(PO_4)_2$, is dewatered in an FPAKM filter-press. The regenerated solution and filtrate are collected in a tank and then fed to a mechanical filter loaded with dolomite. After the filtration, the solution (now containing 2 to 4 mg/liter PO_4^{3-}) is neutralized in a tank of hydrochloric acid and fed to regenerate the Na-cationite filter. This closed regeneration cycle results in a no-waste Na-cationization scheme. The wet sediment, a mixture of $Ca_3(PO_4)_2$ and $Mg_3(PO_4)_2$, is used as liquid or solid fertilizer depending on the time of year. The second version of the new wastewater-recovery process calls for the production of homogeneous sediments, i.e., the chemical products $CaSO_4$, $Mg(OH)_2$, and $CaCO_3$. The new recovery process is beneficial both economically and ecologically. Figures 2.

Dust Removal and Pelletizing of Finely Disperse Carbon Materials and Waste

937D0029F Moscow IZVESTIYA VYSSHIKH UCHEBNYKH ZAVEDENIY: CHERNAYA METALLURGIYA in Russian No 4, Apr 92 pp 72-75

[Article by V.M. Dinelt, K.A. Cherepanov, V.I. Livenets, Siberian Metallurgical Institute; UDC 669.046.004.8]

[Abstract] The high value of many waste and secondary materials which in a number of cases is equal to that of the original raw material and the demand for developing waste-free production processes necessitate attempts to develop methods of waste recovery both at the source or at the location of its likely use as a new raw material. The issue of recovering finely disperse materials, e.g., carbon-bearing, by capturing dust and pelletizing them is addressed; the difficulty of transporting such materials is noted. The dust trapping and pelletizing practices are illustrated using the example of carbon-bearing waste recovery from the graphitization furnaces at the Novosibirsk Electrode Works (NovEZ) and heat-treated coal charge of the Western Siberian Integrated Iron and Steel Works (SZMK). The results of the proximate and mesh analyses of the NovEZ waste and ZSMK charge are summarized, and the pelletizing and dust removal procedures are outlined in detail. The inexpediency of using water for binding dust prompted an addition of small amounts of diesel fuel to the heat-treated charge and the use of coal tar. The averaged results of the carbon-bearing waste granulation with the help of various binders, such as sodium silicate solution, sulfite yeast slop, and "briquetting agents" are tabulated. Preference is given to granulation as being simpler and more efficient. The findings confirm the possibility of decreasing and even eliminating the dust formation during the shipping of finely disperse carbon-bearing materials and waste using two technologies: treatment with various liquids in order to coagulate the dust fractions and pelletizing of the finely disperse fraction by granulation and briquetting. The proposed methods have been implemented at the Novosibirsk Electrode Works. Tables 2.

On Issue of Industrial Discharge Dispersion of Metallurgical Plants in Environment

937D0030I Moscow IZVESTIYA VYSSHIKH UCHEBNYKH ZAVEDENIY: CHERNAYA METALLURGIYA in Russian No 3, Mar 92 pp 82-85

[Article by Yu.M. Pogosbekyan, Moscow Automotive-Highway Institute; UDC 669.013.5:502.7]

[Abstract] The urgency of predicting the environmental contamination with harmful substances released by foundries as a function of the operating conditions, the degree of industrial discharge purification, atmospheric stability, and the terrain relief necessitated the measurement of the toxic substance discharge rate and the development of mathematical models of the harmful substance dispersion in the atmosphere. The harmful substance transfer and generation rate equations are derived and solved by the Green's function method. A graphic model of contamination dispersion from a point source is drawn, and a schematic mathematical description of the gas deflection from the earth surface is plotted. For illustration, carbon monoxide dispersion in the atmosphere from a foundry with a 60 m smokestack and a 100,000 ton/year annual output is calculated at a discharge rate of 140 g x m^3/s and a wind velocity of 6 m/s. The method can also be used for analyzing the environmental contamination by metallurgical and automotive plants. Figures 2; tables 1; references 6: 4 Russian, 2 Western.

22161
24
NTIS
ATTN PROCESS 103
5285 PORT ROYAL RD
SPRINGFIELD VA 22161

BULK RATE
U.S. POSTAGE
PAID
PERMIT NO. 352
MERRIFIELD, VA.

This is a the policies, views, or attitudes of the U.S. Government. Users of this publication may cite FBIS or JPRS provided they do so in a manner clearly identifying them as the secondary source.

Foreign Broadcast Information Service (FBIS) and Joint Publications Research Service (JPRS) publications contain political, military, economic, environmental, and sociological news, commentary, and other information, as well as scientific and technical data and reports. All information has been obtained from foreign radio and television broadcasts, news agency transmissions, newspapers, books, and periodicals. Items generally are processed from the first or best available sources. It should not be inferred that they have been disseminated only in the medium, in the language, or to the area indicated. Items from foreign language sources are translated; those from English-language sources are transcribed. Except for excluding certain diacritics, FBIS renders personal names and place-names in accordance with the romanization systems approved for U.S. Government publications by the U.S. Board of Geographic Names.

Headlines, editorial reports, and material enclosed in brackets [ ] are supplied by FBIS/JPRS. Processing indicators such as [Text] or [Excerpts] in the first line of each item indicate how the information was processed from the original. Unfamiliar names rendered phonetically are enclosed in parentheses. Words or names preceded by a question mark and enclosed in parentheses were not clear from the original source but have been supplied as appropriate to the context. Other unattributed parenthetical notes within the body of an item originate with the source. Times within items are as given by the source. Passages in boldface or italics are as published.

SUBSCRIPTION/PROCUREMENT INFORMATION

The FBIS DAILY REPORT contains current news and information and is published Monday through Friday in eight volumes: China, East Europe, Central Eurasia, East Asia, Near East & South Asia, Sub-Saharan Africa, Latin America, and West Europe. Supplements to the DAILY REPORTs may also be available periodically and will be distributed to regular DAILY REPORT subscribers. JPRS publications, which include approximately 50 regional, worldwide, and topical reports, generally contain less time-sensitive information and are published periodically.

Current DAILY REPORTs and JPRS publications are listed in *Government Reports Announcements* issued semimonthly by the National Technical Information Service (NTIS), 5285 Port Royal Road, Springfield, Virginia 22161 and the *Monthly Catalog of U.S. Government Publications* issued by the Superintendent of Documents, U.S. Government Printing Office, Washington, D.C. 20402.

The public may subscribe to either hardcover or microfiche versions of the DAILY REPORTs and JPRS publications through NTIS at the above address or by calling (703) 487-4630. Subscription rates will be provided by NTIS upon request. Subscriptions are available outside the United States from NTIS or appointed foreign dealers. New subscribers should expect a 30-day delay in receipt of the first issue.

U.S. Government offices may obtain subscriptions to the DAILY REPORTs or JPRS publications (hardcover or microfiche) at no charge through their sponsoring organizations. For additional information or assistance, call FBIS, (202) 338-6735,or write to P.O. Box 2604, Washington, D.C. 20013. Department of Defense consumers are required to submit requests through appropriate command validation channels to DIA, RTS-2C, Washington, D.C. 20301. (Telephone: (202) 373-3771, Autovon: 243-3771.)

Back issues or single copies of the DAILY REPORTs and JPRS publications are not available. Both the DAILY REPORTs and the JPRS publications are on file for public reference at the Library of Congress and at many Federal Depository Libraries. Reference copies may also be seen at many public and university libraries throughout the United States.